

CHAPTER 2

HEPATOCYTE PROLIFERATION AND THERMALLY INDUCED CELL DETACHMENT ON NON-WOVEN PP, PET AND NYLON THREE-DIMENSIONAL SCAFFOLDS

2.1. INTRODUCTION

Historically, anchorage-dependent cells have been cultured on flat surfaces of glass and, more recently, on modern tissue culture plastics. Once the cultured cells have reached the desired level of confluency, they are sub-cultured or passaged. The process of dissociating the cells from the surface of the tissue culture plastic typically requires the use of enzymes such as trypsin, collagenase or pronase. Trypsin, an endopeptidase produced in the gastro-intestines of mammals, is most commonly used. All three enzymes act by digesting proteins, thus during the process of cell dissociation, they modify surface exposed cellular proteins and cell membrane composition. This process has a detrimental effect on the cells if one wishes to use them downstream in immunological or physiological assays. Additionally, ECM components and cell-cell junctions are also digested by trypsin.

Non-enzymatic methods for cell dissociation include solutions containing ethylenediaminetetraacetic acid (EDTA), cell scraping and cell freezing. Cell scraping is typically conducted using a rubber cell scraper in the culture flask in a pre-warmed, balanced salt solution and then dissociating the cells by gentle vortexing or trituration (repeated, gentle pipetting); this results in viable and intact cells. Freezing is another alternative for cell harvesting and although cells are not usually viable after freezing, many membrane characteristics and immunological properties remain intact. This technique is often used for harvesting protease sensitive biological materials rather than whole cells (102).

Over the past three decades, extensive research has been conducted on the use of thermoresponsive, “smart” polymers used in 2D cell culturing to allow non-invasive harvesting of cells and cell sheets. The temperature-sensitive polymer, poly(*N*-isopropylacrylamide) (PNIPAAm) has been covalently grafted onto 2D polystyrene cell culture tray surfaces to facilitate cell attachment and trypsin-independent cell release induced by a temperature change (103).

Chapter 2: Hepatocyte proliferation and thermally induced cell detachment on 3D scaffolds

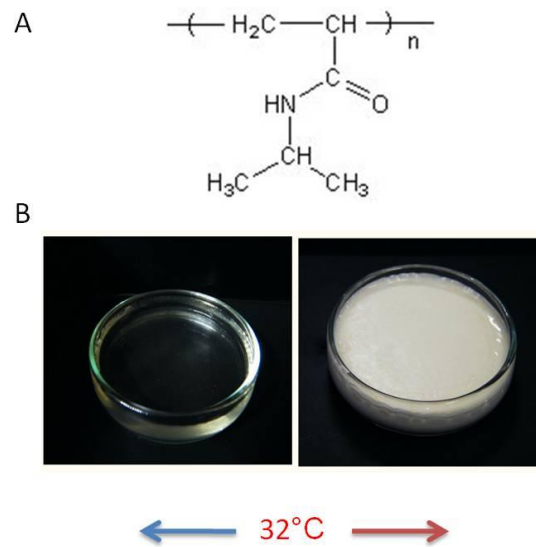


Figure 2.1. Poly(*N*-isopropyl acrylamide). **A.** The structure of the *N*-isopropyl acrylamide monomer. **B.** Poly(*N*-isopropyl acrylamide) below its lower critical solution temperature (LCST, hydrated, hydrophilic) of 32°C and above its LCST (dehydrated, hydrophobic).

PNIPAAm switches reversibly between hydrophobic and hydrophilic states when the temperature crosses its lower critical solution temperature (LCST) of approximately 32°C (Figure 2.1). This is due to the presence of the hydrophilic amide groups and the hydrophobic isopropyl group on its side chain. When the temperature is below the LCST the hydrophilic chains are hydrated and the polymer swells; as the temperature increases past the LCST, the hydrophobic interaction becomes stronger, the balance between hydrophilic/hydrophobic interactions break down, and the polymer collapses (104). This allows cells to attach onto the PNIPAAm surface at 37°C when the surface is hydrophobic while spontaneously releasing cells from the hydrophilic surface at 25°C (103). The major advantage of using PNIPAAm in 2D cell culture is that cells are non-invasively harvested as intact cell sheets with critical cell surface proteins, growth factor receptors, and cell-to-cell junction proteins remaining intact (Figure 2.2) (105-107).

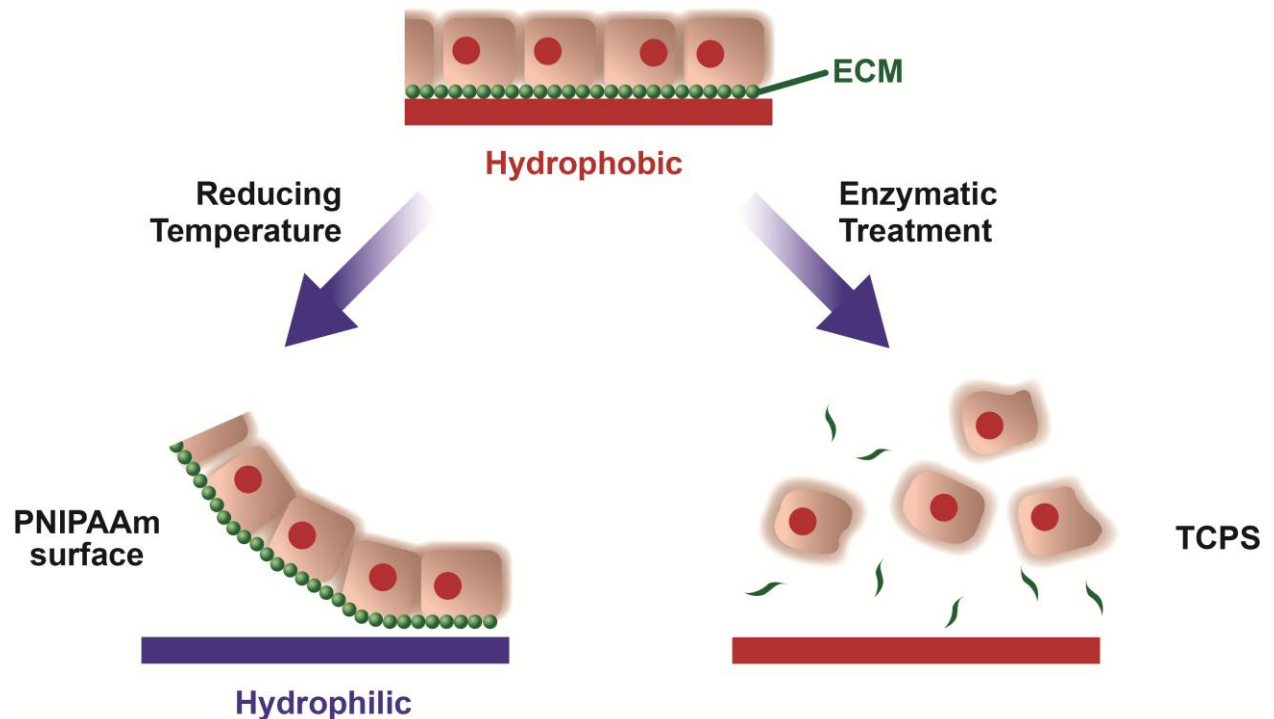


Figure 2.2. Temperature-responsive culture dishes. During cell culture, cells deposit extracellular matrix (ECM) molecules and form cell-to-cell junctions (top). Cells harvested from temperature-responsive dishes (left) are recovered as intact sheets along with their deposited ECM (green), by simply reducing the temperature. With typical proteolytic harvesting of cells growing on tissue culture poly(styrene) (TCPS) by trypsin, both ECM (green) and cell-to-cell junction proteins are degraded for cell recovery. Figure modified from (108).

As iterated in Chapter 1, although 2D cell culture is convenient for routine work, researchers are turning to 3D cell culture for more accurate, physiologically representative information on the way their cells behave and respond to stimuli. Cells can now be routinely cultured in 3D. However, the means of harvesting the cells from the scaffolds is more challenging than in 2D. To this extent, many of the 3D scaffolds currently manufactured are either bio-degradable or require the use of salts to dissolve the scaffold, which may negatively impact the cells they contain. This study, therefore, proposes combining 3D cell culture technology with the temperature responsive polymer PNIPAAm, shown to allow non-invasive cell release in 2D, to create a novel 3D scaffold for simple 3D cell culture and easy, non-invasive cell harvesting.

2.1.1. Scaffold selection

Selection of the type of 3D scaffold for grafting with PNIPAAm was thoroughly considered. In order to create a 3D matrix within which cells would be seeded and proliferate eliminated the idea of making the whole scaffold out of PNIPAAm hydrogel. Firstly, it would have been too expensive and secondly, above the polymer's LCST, it is in a dehydrated conformation that would result in the whole gel collapsing at 37°C under standard cell culture conditions (109).

Chapter 2: Hepatocyte proliferation and thermally induced cell detachment on 3D scaffolds

Grafting PNIPAAm onto another hydrogel polymer was considered but cell retention would be problematic. A hydrogel grafted with PNIPAAm would possibly not release the cells when one lowered the temperature as the cells may become trapped in the hydrogel due to pore size distribution and tortuosity issues. Using a 'soluble' hydrogel was also considered; once the cells have populated the hydrogel it is dissolved to recover the cells. However, that would have made the 3D system not easily re-usable, and not suited for semi-continuous cell production in a bioreactor should the need arise.

Non-hydrogel scaffolds such as foams were also considered, but foams are typically very dense, with lower percentage open pores or free volume and have higher tortuosity than for example, non-woven scaffolds. This study required a scaffold where pore size distribution could be varied over a substantial range, and non-woven scaffolds allow this, whilst having a high percentage free volume. It was also thought that a non-woven scaffold would possess the best chance of releasing cells easily from the scaffold due to their interconnected open pore structure. In addition, non-woven scaffolds can be cut or rolled into any shape required.

2.1.2. Cell culture automation

In parallel to the increasing demand for cells that more closely mimic *in vivo* characteristics, bench scientists to large-scale bio-manufacturers are turning to solutions that allow hands-free growth, maintenance, and monitoring of cells for just-in-time delivery of cells into downstream applications. Furthermore, studies have shown that cells grow significantly better under dynamic culture conditions as a result of continuous cycling of nutrients as well as the removal of metabolic wastes (110). In some instances, the sheer force produced by the flowing medium can act as a mechanical stimuli signal that further promotes stem cell differentiation towards certain cell-lineages (110). The use of a non-destructive, three-dimensional automated cell culturing system could potentially revolutionize the cell culture fraternity and many large corporations such as Hamilton are investing in this technology (111).

2.1.3. Objectives

This chapter describes the biological contributions to a transdisciplinary approach to create thermoresponsive, non-woven scaffolds amenable to automated cell culturing. In this collaborative effort, scaffold selection and fabrication was performed by Rajesh Anandjiwala (Materials Science and Manufacturing (MSM), CSIR). Subsequently, in this study, these

Chapter 2: Hepatocyte proliferation and thermally induced cell detachment on 3D scaffolds

scaffolds were grafted with PNIPAAm and tested for their ability to functionally support cell growth in 3D and allow non-invasive release of the cells from the matrix.

Based on the identified system functional requirements as well as normal bioreactor perfusion circuit design criteria, a preliminary design of an automated cell culture system was developed by Mr Kobus van Wyk of Blue Line Designs (Pretoria, South Africa). Here, the selected thermoresponsive, non-woven fabrics tested for cell growth and release were further analysed in the automated cell culture device for cell proliferation and thermally induced harvesting.

2.2. MATERIALS AND METHODS

2.2.1. Scaffold fabrication

Three different non-woven polymer scaffolds were investigated in this study as substrates for cell proliferation. Fabrics made from poly(propylene) (PP) and poly(ethylene terephthalate) (PET) non-woven polymers with a median flow pore (MFP) size of 150-300 μm were developed based on needle-punching technology. Needle-punched non-woven fabrics are created by mechanically orienting and interlocking the fibres of a spun-bonded or carded web. This mechanical interlocking is achieved with thousands of barbed felting needles repeatedly passing into and out of the web. The non-woven mats used as scaffolds were thermo-fused at 145°C (PP) and 180°C (PET), in order to prevent the dissociation of the fibres during cell culture. Nylon non-woven scaffolds with pores sizes in the range of 40-80 μm were developed due to the lower fibre density of the nylon compared to PP and PET fibres, and thermofused at 200°C. The non-woven scaffolds were manufactured and characterised by Rajesh Anandjiwala (MSM, CSIR) for porosity, water permeability, compressibility, fabric density, tensile strength, area weight and thickness (data not shown).

2.2.2. Grafting methods

PP, PET and nylon non-woven scaffolds were grafted with PNIPAAm using a solution free-radical polymerisation (SFRP) technique by Avashnee Chetty (MSM, CSIR). Briefly, the grafting methods investigated involved swelling of pure (or functionalised) non-woven scaffolds in an initiator solution followed by SFRP in an aqueous NIPAAm monomer solution with heat activation (70°C or 50°C). Two functionalisation methods were investigated prior to grafting, i.e. oxyfluorination (performed using a proprietary method at Pelchem (Pty) Ltd, South Africa) or a chemical oxidation method using ammonium persulphate (APS). Grafting of PNIPAAm onto the surface of the fibres was confirmed by attenuated total reflection-fourier transform infrared spectroscopy (ATR-FTIR), differential scanning calorimetry (DSC), X-ray photoelectron spectroscopy (XPS) and scanning electron microscopy (SEM). Table 2.1 summarises the various scaffolds received from MSM (CSIR) for testing.

Table 2.1. Non-woven scaffolds used for this study. The various non-woven scaffolds both control (Cont) and grafted (*g*-NIPAAm) received from Avashnee Chetty (MSM, CSIR) for cell culture testing.

Scaffold material	Scaffold name	Mean pore size (µm)
Control scaffolds (not grafted)		
Poly(propylene)	PP-Cont	127
Poly(ethylene terephthalate)	PET-Cont	127
Nylon	Nylon-Cont	40-80
Grafted scaffolds		
Poly(propylene)	PP- <i>g</i> -NIPAAm-1	127
	PP- <i>g</i> -NIPAAm-1a	127
	PP- <i>g</i> -NIPAAm-2	127
	PP- <i>g</i> -NIPAAm-A	127
	PP- <i>g</i> -NIPAAm-B	127
	PP- <i>g</i> -NIPAAm-B1	100
	PP- <i>g</i> -NIPAAm-B2	150
	PP- <i>g</i> -NIPAAm-B3	200
Poly(ethylene terephthalate)	PET- <i>g</i> -NIPAAm-2	127
	PET- <i>g</i> -NIPAAm-A	127
	PET- <i>g</i> -NIPAAm-B	127
Nylon	Nylon- <i>g</i> -NIPAAm-A	40-80
	Nylon- <i>g</i> -NIPAAm-B	40-80

A commercially available 3D culturing system, AlgiMatrix™ (Gibco®, Invitrogen Corporation, Carlsbad, California, USA), was included in the study to serve as a control in order to benchmark our scaffolds' performance for cell proliferation. The AlgiMatrix™ 3D system is based on hydrogel technology and has been used to proliferate hepatocytes (112).

2.2.3. Cell-scaffold interaction

HC04 (MRA-156, MR4, ATCC® Manassas, Virginia) and HepG2 (ATCC HB-8065™, ATCC®) hepatocyte cell-lines were used in the study. HC04 cells are human hepatocytes immortalised by Sattabongkot *et al.* from healthy, human primary liver cells to support the *in vitro* development of human malaria species (113). HepG2 cells are human hepatocellular liver carcinoma cells routinely used worldwide for *in vitro* liver studies. Scaffolds of size 5 x 5 x 3 mm were sterilised in 70% ethanol for 1 h, rinsed three times in 1x PBS and allowed to dry in a laminar hood. The scaffolds were soaked overnight at 37°C in the cell culture media specific for

Chapter 2: Hepatocyte proliferation and thermally induced cell detachment on 3D scaffolds

the cell-line used (see below), to reduce any surface tension effects (114) as well as to ascertain whether the scaffolds had been effectively sterilised prior to seeding the non-woven scaffolds with the hepatocytes.

HepG2 cells were cultured in Dulbecco's Modified Eagle Medium (DMEM, Lonza Walkersville, Inc. Maryland, USA) with 2 mM L-glutamine and supplemented with 10% (v/v) foetal calf serum (FCS), 1% (v/v) antibiotics (10000 unit/10 mg/mL Pen/Strep, Sigma-Aldrich Chemie, GmbH, Steinheim, Germany). HC04 cells were cultured in 1:1 DMEM:Hams F12 media (Lonza) with 2 mM L-glutamine and supplemented with 10% (v/v) FCS, 100 g/mL penicillin and 10 µg/mL streptomycin (Sigma-Aldrich Chemie). The cells were cultured in T75 culture flasks (Nunc, Roskilde, Denmark) in a humidified incubator at 37°C and 5% CO₂ (standard conditions) and were subcultured once or twice a week depending on the confluence. When the cells were approximately 70% confluent they were trypsinised and resuspended at the correct concentration for seeding onto the scaffold. Briefly, the cell culture media was aspirated from the HC04 and HepG2 hepatocytes growing in culture flasks and the cell layer was gently rinsed with phosphate buffered saline (PBS, pH 7.4, Lonza Walkersville) to remove any residual cell culture media containing FCS, which inhibits the action of trypsin. The cells were covered with a thin layer (approximately 10 mL) of trypsin-versene (EDTA) (Lonza Walkersville) and incubated for 5 min at 37°C whereafter 20 mL of culture media was added to the detached cells to inactivate the trypsin. The cells were added to a 50 mL centrifuge tube (BD Biosciences, San Jose, California), pelleted by centrifugation at (50g) and the supernatant was aspirated off the cell pellet. Viable cells were counted using trypan blue dye exclusion on a haemocytometer and the hepatocytes were resuspended to a concentration of 1×10^6 cells/mL. A 200 µL aliquot of this was gently dripped onto each of the non-woven scaffolds (Table 2.1) and Algimatrix™ scaffolds in a 96-well plate, resulting in a final concentration of 2×10^5 cells seeded onto each scaffold.

The scaffolds were incubated at 37°C for 2 h to allow cell attachment. Thereafter, the scaffolds were removed from the 96-well tissue culture plate using sterile tweezers and individually placed into the well of a 12-well tissue culture plate with 2 mL cell-specific media and cultured in a humidified incubator under standard conditions. Scaffolds containing the HepG2 and HC04 hepatocytes were maintained in culture for a period of 21 days with media changes performed every 48 hours post inoculation (hpi).

2.2.4. Cell viability and proliferation

2.2.4.1. AlamarBlue® assay

The AlamarBlue® (AB, Invitrogen Molecular Probes®, Eugene, Oregon, USA) cell viability reagent functions as a cell health indicator. It was used to estimate the number of viable cells growing in the 3D scaffold (*in situ*) without the need to release the cells from the scaffolds (115, 116). The active ingredient is resazurin, a non-toxic cell-permeable compound; resazurin is a blue, non-fluorescent compound which, upon entering a healthy cell, is reduced to resorufin that is a red, highly fluorescent compound.

A standard curve for the AB assay was generated in order to determine cell proliferation by correlating a known cell number with the fluorescent intensity of the solution after an optimised incubation time. Standard curves were generated for both the HepG2 and HC04 cell-lines in a 24-well tissue culture plate. Cell suspensions were prepared as described in section 2.2.3 to an initial concentration of 2×10^6 hepatocytes/mL, from which the cells were serially diluted (1:2) in cell culture media thus generating a cell concentration range from 2×10^6 hepatocytes/mL to 3.125×10^4 hepatocytes/mL (117). The cell dilutions (500 μ L each) were seeded into triplicate wells of the 24-well tissue culture plate and incubated at 37°C. After an initial 2 - 3 h attachment period, the culture media was removed and the cells were re-fed with 450 μ L fresh, pre-warmed media containing 50 μ L (10% v/v final concentration) AB. After an optimised incubation period of 30 min at 37°C in the dark, 100 μ L of the reduced media from each well was transferred in duplicate to individual wells of a black-walled 96-well plate and the fluorescence was read using a microplate reader (Tecan GENios, Tecan Group Ltd. Männedorf, Switzerland) at excitation and emission wavelengths of 520 nm and 590 nm, respectively. The series of cultures with known cell numbers were correlated to their respective fluorescence values to generate the standard curve.

All of the scaffolds listed in Table 2.1 and the AlgiMatrix™ alginate scaffolds were subsequently seeded with either 200 μ L of a 1×10^6 cells/mL HC04 cell suspension or with HepG2 cells. Duplicate samples of 6 independent biological replicates (n=6) were used for each scaffold. The scaffolds were placed in into the wells of low cell-binding 6-well tissue culture plates with 3 mL of specific cell culture media for each cell type. The cells on the scaffolds were maintained under standard conditions and the media changed every 48 hpi. The AB assay was performed using the scaffolds 0, 3, 7, 11, 15 and 21 days post inoculation (dpi). These time points were selected based on previous work by Mandal and Kundu (116), Shor *et al.* (115) and Wagner *et*

Chapter 2: Hepatocyte proliferation and thermally induced cell detachment on 3D scaffolds

al. (114). The day 0 time point served as a leak test and was used to ascertain how many cells were retained in the different scaffolds after 2 hpi. Five scaffolds per treatment were then transferred individually to the wells of a 24-well tissue culture plate containing 450 μL of fresh, pre-warmed cell culture media with 50 μL (10% v/v) AB. As a negative control (blank), 10% AB was added to media without cells. The cells were re-incubated at 37°C for 30 min in the dark, after which the plates were gently swirled to ensure equal mixing of the dye solution. Subsequently, 100 μL of the media was aliquoted in duplicate into the wells of a black-walled 96-well plate and the fluorescence was read as described above. The blank values were subtracted from the fluorescent values and the data were converted to viable cell number per scaffold using the standard curve generated above. The media was removed from the wells in which the scaffolds were placed and these were frozen at -70°C for subsequent DNA quantification.

2.2.4.2. DNA quantification using Hoechst 33258

Hoechst 33258 (Invitrogen Molecular Probes®) is a bisbenzimidazole DNA intercalator which binds to the AT rich regions of double stranded DNA. Hoechst 33258 excites in the near UV (350 nm) and emits in the blue (450 nm) regions.

In order to generate standard curves from crude cell lysates, as outlined by Rago *et al.* (118), the HC04 and HepG2 cell-lines were seeded into 24-well tissue culture plates as described above. After cell adhesion to the tissue culture plates, the medium was removed, cells were washed once with distilled water to remove residual cell culture media as well as any dead cells and 500 μL distilled water was subsequently added. The cells were incubated at 37°C for 1 h followed by three freeze-thaw cycles at -70°C to lyse the cells. Equal volumes of the cell lysate and Hoechst 33258 (20 $\mu\text{g}/\text{mL}$) were added to a total volume of 200 μL in a black 96-well plate and mixed well. A negative control (blank) was generated by adding the working dye solution to a sample of distilled water without cells. Fluorescence was measured and the blank subtracted from the values obtained to generate a standard curve as described above.

After establishment of standard curves, DNA quantification was performed on scaffolds, frozen away from section 2.2.4.1. by the addition of 500 μL distilled water to wells containing the scaffolds and incubation at 37°C for 1 h. This was then followed by three freeze-thaw cycles to lyse the cells on the scaffolds including continuous mixing (by swirling the plates to mix the liquid content) throughout. Equal volumes of the cell lysates and Hoechst 33258 (20 $\mu\text{g}/\text{mL}$) were added in duplicate to the wells of a black-walled 96-well plate and fluorescence measured

Chapter 2: Hepatocyte proliferation and thermally induced cell detachment on 3D scaffolds

as described above. A blank was included to serve as a negative control and was subtracted from the fluorescent values obtained. The number of viable cells per scaffold was calculated by extrapolation from the standard curve.

2.2.5. Imaging cell-scaffold-interaction

The HC04 and HepG2 cells growing on the scaffolds were visualised with fluorescent microscopy using fluorescein diacetate (FDA, Sigma-Aldrich Chemie) to monitor cell attachment and morphology on 3, 7, 11, 15 and 21 dpi (112). The non-specific esterase activity in the cytoplasm of viable cells converts non-fluorescent FDA to fluorescein, a green fluorescent dye. FDA was diluted to 5 mg/mL in acetone. Of this, a 1:250 dilution in 1x PBS was incubated with cells on the scaffolds (enough to cover the scaffold) for 5 min, after which the cells were gently rinsed in PBS to remove any residual dye. Both the top and bottom of the scaffolds were viewed for cell attachment at the days mentioned above at 40x magnification using a standard fluorescence microscope (Olympus BX41, Olympus Microscopy, Essex, UK) equipped with a 490 nm bandpass filter with a 510 nm cut-off filter for fluorescence emission.

2.2.6. Hepatocyte metabolic activity measurement

The production of albumin is often used as an indicator of hepatocyte metabolic activity. Levels of albumin were determined using the Albumine Fluorescence Assay Kit (Sigma-Aldrich Chemie) based on an established method which uses Albumin Blue (119). Albumin Blue is an anionic fluorescent probe that binds to albumin in a specific way to undergo strong fluorescent enhancement with an excitation and emission wavelength of 600 and 630 nm, respectively. Specific levels of albumin secretion were normalised to total protein levels as determined by a standard Bradford assay (5).

2.2.6.1. Bradford standard curve

The Bradford assay is a protein determination method that involves the binding of Coomassie Brilliant Blue G-250 dye to proteins (120). Upon binding to protein, the doubly protonated red cationic form detected at 470 nm is converted to a stable unprotonated blue form that is detected at 595 nm. A standard curve was created using a 250 μ L microplate assay with a bovine gamma-globulin standard set with seven concentrations of gamma globulin (2, 1.5, 1, 0.75, 0.5, 0.25 and 0.125 mg/mL). Briefly, 5 μ L of the gamma globulin standard dilutions and 250 μ L of the 1x dye reagent were combined, in triplicate, in individual wells of a 96-well

Chapter 2: Hepatocyte proliferation and thermally induced cell detachment on 3D scaffolds

microplate; a blank consisting of only the 1x dye reagent was also included. The samples were incubated at room temperature for 5 min and the absorbance measured at 595 nm on a Bio-Tex EL808 plate reader (A.D.P, Weltevreden Park, South Africa). The values from the blank samples were subtracted from the absorbance values and the data from the replicates were averaged. A standard curve was created by plotting the 595 nm values against their corresponding concentration in $\mu\text{g/mL}$.

2.2.6.2. Albumin assay

A standard curve was generated using the calibrator solution in the Albumine (human) Fluorescence Assay Kit (Sigma-Aldrich Chemie). The calibrator solution (human albumin stock solution) of 2000 mg/L was diluted to final concentrations of 2, 10, 30, 100 and 200 mg/mL in distilled water. Calibrator solution (35 μL of each dilution) was mixed with 175 μL assay reagent and the fluorescence was read on a microplate reader (Tecan GENios) at excitation and emission wavelengths of 600 and 630 nm, respectively.

PP-Cont (un-grafted scaffolds, mean pore size of 200 μm , Table 2.1) were punched into disks (15 mm in diameter and 3 mm thick, $n=3$), seeded with 1.5×10^6 HC04 or HepG2 hepatocytes and cultured for 21 dpi; media changes were performed every 24 h. Culture supernatant samples were collected every 24 hpi for albumin quantification on days 3, 7, 10, 14 and 21 dpi. The 24 h culture supernatant from a 70% confluent 75 cm^2 flask of HC04 or HepG2 hepatocytes was used as the 2D comparison. Sample solution (35 μL each in triplicate) was mixed with 175 μL assay reagent and the fluorescence was read on a microplate reader. The fluorescent values were blanked to a well containing only the assay reagent. Total albumin was calculated by extrapolation from the standard curve and normalised to total protein in the media as determined by the Bradford assay. Statistical analysis was performed using a paired t-test of unequal variance where $P<0.01$ and $P<0.05$.

2.2.7. Cytochrome P450 mRNA expression

PP-Cont non-woven scaffolds with a mean pore size of 200 μm , seeded with HC04 hepatocytes (as in section 2.3.3) were frozen away on 10, 14 and 21 dpi. Scaffolds seeded with HepG2 hepatocytes were frozen away at 21 dpi. To investigate the effect of scaffold pore size and/or grafting on gene expression, PP-*g*-PNIPAAm scaffolds with mean pore sizes of 100, 150, 200 μm (PP-*g*-PNIPAAAM-B1, PP-*g*-PNIPAAAM-B2, PP-*g*-PNIPAAAM-B3; Table 2.1) were seeded with HC04 hepatocytes and frozen away on 21 dpi. Hepatocytes growing in a control 75 cm^2 cell

Chapter 2: Hepatocyte proliferation and thermally induced cell detachment on 3D scaffolds

culture flask were harvested via trypsination at 70% confluence and frozen at -80°C until further use.

2.2.7.1. RNA extractions

RNA was isolated under RNase-free conditions according to the method described by Clark *et al.* (121), a method that utilises both Tri-Reagent and the RNeasy kit (Qiagen GmbH, Hilden, Germany). The monophasic, phenol/guanidine thiocyanate solution in TRI-Reagent inhibits RNase activity and lyses the sample material. The homogenate is then separated into aqueous and organic phases by the addition of chloroform followed by centrifugation. RNA partitions in the aqueous phase, DNA in the interphase and proteins in the organic phase. The RNA was then precipitated from the aqueous phase with ethanol (EtOH).

Total RNA was extracted from the frozen hepatocytes on 3D scaffold and cell pellets from 2D cell culture using the RNeasy kit (Qiagen). The hepatocytes on the 3D scaffolds and the cell pellets were fully defrosted to room temperature and a volume of 600 µL RLT buffer (lysis buffer, proprietary) was added to each sample and mixed; this mixture was centrifuged at 7000g through a Qia-Shredder column (Qiagen) for physical cell rupture. The flow-through was collected and mixed with 600 µL TRI-reagent in a 2 mL microfuge tube. After a 5 min incubation at room temperature, 400 µL chloroform was added, vortexed and incubated at room temperature for 10 min. The samples were collected by centrifugation at 7000g for 15 min and the upper aqueous phase of each was transferred to a clean tube without disturbing the interphase. The RNA was precipitated with 700 µL 70% (v/v) EtOH, loaded onto RNeasy columns and centrifuged for 15 s at 8000g. The RNA was washed with 350 µL buffer RW1 (proprietary) followed by an on-column DNase treatment using 27 units DNase 1 (Qiagen) to degrade any residual contaminating DNA. The RNA was then washed again with buffers RW1 and RPE following which the column was placed in a clean microfuge tube and RNA eluted in 30 µL of RNase-free water by incubation at room temperature for 3 min and centrifugation at 8000g for 1 min and stored at -70°C. The concentration of RNA was determined by measuring the absorbance at 260 nm by UV spectrophotometry with a NanoDrop-1000 (Thermo Fisher Scientific, Waltham, MA, USA). An absorbance of 1 unit at 260 nm corresponds to 40 µg/mL RNA. The ratio between the absorbance values at 260 and 280 nm gives an estimate of RNA purity; pure RNA has an A₂₆₀/A₂₈₀ ratio of 1.9-2.1.

2.2.7.2. cDNA synthesis and qRT-PCR

First strand cDNA was synthesised using the high-capacity RNA-to-cDNA Kit (Life Technologies Corporation, Carlsbad, CA, USA) according to kit instructions. The High Capacity RNA-to-cDNA Kit is a streamlined reverse transcription kit designed for optimum performance with the TaqMan® Gene Expression Master Mix, Power SYBR® Green PCR Master Mix and other PCR enzymes. SYBR® Green is an asymmetrical cyanine dye used to detect polymerase chain reaction (PCR) products by binding to double-stranded DNA formed during the PCR reaction. As the PCR progresses, more PCR product is created; since the SYBR® Green dye binds to all double-stranded DNA, the result is an increase in fluorescence intensity proportionate to the amount of PCR product produced.

The RNA-to-cDNA Kit includes 20x Enzyme Mix (Multiscript MuLV reverse transcriptase and RNase inhibitor protein) and 2X RT Buffer Mix (includes dNTPs). RNA (2 µg) was added to 2X RT buffer and 20x enzyme mix. The mixture was incubated at 37°C for 60 min followed by 5 min at 95°C to stop the enzymatic reaction; the cDNA was stored at -20°C.

Cytochrome P450 (CYP) 2C19, 2C9, 1A2, 2D6, 3A4 and 3A5 mRNA expression levels were determined using quantitative real time-PCR (qRT-PCR). The qRT-PCR was conducted according to manufacturer's instructions: each 20 µL reaction contained the following reagents: 1X Power SYBR® Green PCR Master Mix II (Life Technologies), 200 nM of both the forward and reverse primers, 10 µg cDNA template and the balance up to 20 µL, nuclease-free water. The thermal cycles were as follows: 95 °C for 10 min followed by 40 cycles of denaturing at 95°C for 15 s and extension at 60°C for 1 min. The samples were run and analysed on a 7500 Fast Real-Time PCR System (Applied Biosystems, Forster City, CA, USA). A melting curve analysis was performed to ensure that there was not more than one PCR product being produced in the reaction. Relative quantification of gene expression levels was determined using the comparative Ct method ($2^{-\Delta\Delta C_t}$) (122) and normalised to the β -actin gene (97). Statistical analysis was performed as described in 2.2.6.2.

2.2.8. Thermal release of cells from the various scaffolds.

Hepatocytes were cultured on all grafted scaffolds (5x5x3 mm, Table 2.1) for 10 days. The scaffold had been ethanol sterilised as outlined in section 2.2.3 and a duplicate set of scaffolds were autoclaved (121°C for 20 min); this was done to assess if the method of sterilisation had an effect on the functionality of the grafted PNIPAAm layer. On day 10 post inoculation the

Chapter 2: Hepatocyte proliferation and thermally induced cell detachment on 3D scaffolds

scaffolds were gently rinsed in sterile PBS pre-warmed to 37°C to remove loose or dead cells and were placed (3 per well) into a 6-well plate containing 2 mL of cooled (20°C) culture media. Nine scaffolds were used per grafting and sterilisation method: three scaffolds which remained in the incubator at 37°C, three at 20°C for 1 h and three at 20°C for 2 h to establish the length of time necessary for temperature-mediated cell detachment; a maximum of 2 h was used as previously described by Canavan *et al.* (123). The cell culture plates containing the scaffolds were periodically agitated by gentle swirling during the incubations, where-after the scaffolds were removed and the released cells on the bottom of the wells photographed under bright field illumination using a 4x objective and an Olympus BX41 microscope fitted with a CC-12 digital camera (Soft Imaging Systems GbmH, Münster, Germany).

2.2.9. Automated cell culture and thermal cell release

An automated cell culture system was proposed as a means to scale up 3D cell culture on the non-woven scaffolds. High-density cell proliferation and non-invasive cell harvesting via thermal release was tested. The automated cell culture system was designed by Kobus van Wyk (Blue Line Designs, Pretoria, South Africa) in consultation with the project team at the CSIR. A prototype automated system was constructed to test the design and specific culture parameters for successful cell proliferation prior to designing a final system for testing (Figure 2.3).

Chapter 2: Hepatocyte proliferation and thermally induced cell detachment on 3D scaffolds

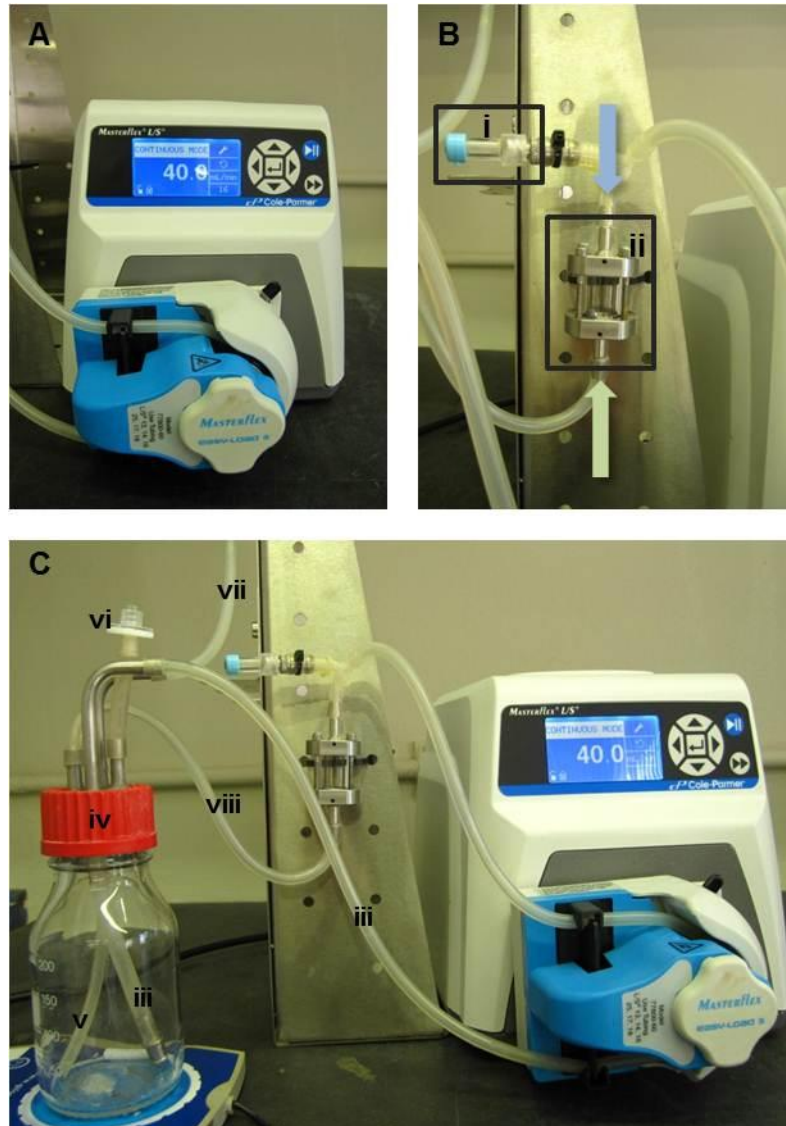


Figure 2.3. The prototype automated cell culture device. **A.** The peristaltic pump. **B.** i: sampling port; ii: the bioreactor (without scaffolds, 4 mL volume); blue and green arrows: media in/out. **C.** The full system, iii: media to bioreactor; iv: media reservoir; v: gas inlet (into the cell culture media); vi: gas vent; vii: gas line from tank; viii: media return line (from the bioreactor).

The prototype automated cell culture device was subsequently tested. Initial experiments were conducted in a small, prototype bioreactor as illustrated in Figure 2.3 to test the suitability of the PP non-woven scaffolds as a scaffold in the continuous perfusion system by optimising several parameters. Pure PP non-woven scaffolds with 200 μm pores were used in the initial experiments. In the final system PP-g-PNIPAAm-B2 (Table 2.1) was selected for use in the bioreactor; the pore size of this scaffold is on average 200 μm . This scaffold with bigger pores was selected such that when the scaffold disks are stacked onto one another there will be more space for released cells to migrate out of the bioreactor for harvesting. Scaffolds with smaller pores may become clogged with cell clusters or the cells clusters may become trapped in the fibre network.

Chapter 2: Hepatocyte proliferation and thermally induced cell detachment on 3D scaffolds

HC04 hepatocytes were seeded (1.5 million cells per non-woven disk of 15 mm diameter) into either the medium reservoir and allowed to circulate through the system where they would become entrapped within the non-woven scaffold or, in a separate experiment, cells were seeded directly into the bioreactor containing the non-woven scaffolds via the sampling port. The media in the reservoir was either static or gently stirred with a small magnetic stirrer. Typically, 3 non-woven scaffolds were used per bioreactor. Hepatocytes were seeded into the bioreactor for 3 h followed by a media change to remove and quantify any cells that had not seeded into the non-woven scaffolds. Media was perfused at 2 mL/min while seeding or allowed, in the case of direct seeding into the bioreactor, to settle without perfusion into the scaffolds.

Media perfusion (axial flow) was tested from either the bottom-up or top-down through the bioreactor containing the non-woven scaffolds to assess which method formed fewer bubbles/air locks and allowed better retention of the hepatocytes within the non-woven scaffolds. Media was perfused at 0.5 mL/min for general cell maintenance.

Media changes were performed when the glucose levels were measured using an Accu-Check Active® glucometer (Roche Pharmaceuticals, Basel, Switzerland) to be below 10 mmol/L approximately half the starting concentration. Once cell seeding and media perfusion parameters were established, cells were seeded into the bioreactor and their proliferation and viability were monitored over a set period of time. Based on the results of the prototype testing, a final system was designed, constructed and tested for its ability to cultivate large numbers of cells. Thermal release of hepatocytes on grafted scaffolds was then assessed in a basic proof-of-concept experiment.

2.3. RESULTS

2.3.1. Grafting methods

Grafting methods that yielded a layer of PNIPAAm on the surface of non-woven scaffolds as verified by Avashnee Chetty (MSM, CSIR) by ATR-FTIR, DSC, XPS and SEM are listed in Table 2.2.

Table 2.2. A summary of successful methods used to achieve a grafted layer of PNIPAAm onto the surfaces of poly(propylene) (PP), poly(ethylene terephthalate) (PET) and nylon non-woven polymers (blue shaded area). The green shaded panel represents scaffolds of different pore sizes grafted as per PP-*g*-PNIPAAm-B and the grey panel summarises the variations of grafting method PP-*g*-PNIPAAm-B to serve as additional controls for thermal release assessment.

Sample Name	Polymer properties			Grafting method				
	Polymer	MFP (µm)	Mass g/m ²	Pre-treatment	Initiator	NIPAAm added	Temp (°C)	Time (h)
PP-Cont	PP	127	-	-	-	-	-	-
PET-Cont	PET	127	-	-	-	-	-	-
Nylon-Cont	Nylon	40-80	-	-	-	-	-	-
PP- <i>g</i> -PNIPAAm-1	PP	127	-	APS ¹	Ceric ion/nitric acid	✓	70	24
PP- <i>g</i> -PNIPAAm-1a	PP	127	-	APS	Ceric ion/nitric acid	✓	50	24
PP- <i>g</i> -PNIPAAm-2	PP	127	-	-	APS	✓	70	24
PET- <i>g</i> -PNIPAAm-2	PET	127	-	-	APS	✓	70	8
PP- <i>g</i> -PNIPAAm-A	PP	127	-	Oxyfluorination ²	APS	✓	70	7
PP- <i>g</i> -PNIPAAm-B (Test 1)	PP	127	-	Oxyfluorination ³	APS	✓	70	7
PET- <i>g</i> -PNIPAAm-A	PET	127	-	Oxyfluorination ²	APS	✓	70	7
PET- <i>g</i> -PNIPAAm-B	PET	127	-	Oxyfluorination ³	APS	✓	70	7
Nylon- <i>g</i> -PNIPAAm-A	Nylon	40-80	-	Oxyfluorination ²	APS	✓	70	7
Nylon- <i>g</i> -PNIPAAm-B	Nylon	40-80	-	Oxyfluorination ³	APS	✓	70	7
PP- <i>g</i> -PNIPAAm-B1	PP	100	200	Oxyfluorination ³	APS	✓	70	7
PP- <i>g</i> -PNIPAAm-B2	PP	150	100	Oxyfluorination ³	APS	✓	70	7
PP- <i>g</i> -PNIPAAm-B3	PP	200	95	Oxyfluorination ³	APS	✓	70	7
Test 2	PP	127	-	Oxyfluorination ³	APS	x	70	7
Test 3	PP	127	-	-	APS	✓	70	7
Test 4	PP	127	-	-	APS	x	70	7

¹Ammonium Persulphate

²Dynamic oxyfluorination 5:95 F:N₂, 3 min exposure

³Static oxyfluorination 20:80 F:N₂ and other gas mixtures, 30 min exposure

2.3.2. Cell viability and proliferation

Since quantifying the number of viable cells in a 3D scaffold is not possible by conventional cell counting methods, the AB assay was used to estimate the number of the cells growing on the scaffold without prior detachment from the scaffold.

The AB assay was performed to determine the number of viable HC04 and HepG2 hepatocytes within the various grafted and control scaffolds. Cell numbers were extrapolated from standard curves generated from serial dilutions of cells in a 24-well plate (Figure 2.4).

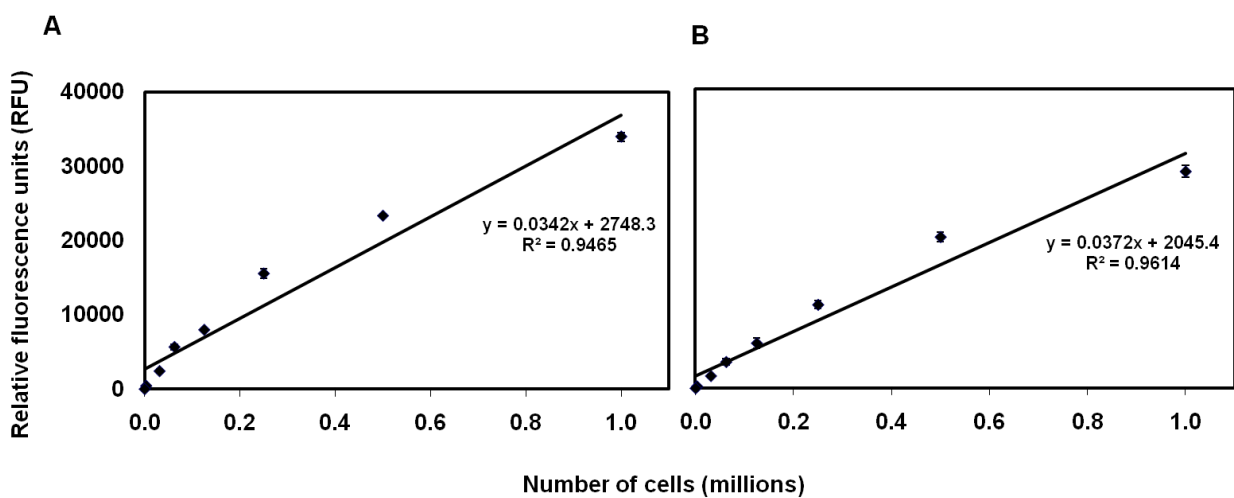


Figure 2.4. AlamarBlue® assay standard curves for HC04 (A) and HepG2 (B) hepatocytes. The standard curves were generated from a pre-determined number of hepatocytes growing in a 24-well tissue culture plate by a 30 min incubation with 10% (v/v) AlamarBlue®. The data are presented as the average of three replicates per cell number plotted against fluorescence \pm standard deviation.

Cells proliferated efficiently as evident from cell number increases over time on all the 3D control and grafted scaffolds (Figure 2.5). The HC04 hepatocytes grown on the PP scaffolds had a first maximum on day 7 with a general decline in numbers on day 11, but cell numbers were observed to recover thereafter. This phenomenon was noted on all scaffolds regardless of the cell-line except in a few instances e.g. HC04 cells growing in the Algimatrix™ alginate scaffolds and grafted nylon scaffolds. On the PP scaffolds, the PP-g-PNIPAAm-1a and PP-g-PNIPAAm-B supported the highest number of HC04 hepatocytes; these results were comparable to the proliferation seen within the Algimatrix™ scaffold. HepG2 hepatocytes growing on PP scaffolds were best supported by PP-g-PNIPAAm-1, PP-g-PNIPAAm-1a and PP-g-PNIPAAm-B; these scaffolds supported more cells than the Algimatrix™ scaffold. HC04 and HepG2 hepatocytes growing on the PET scaffolds were, by comparison, better supported by the Algimatrix™ scaffold as well as the control scaffold. HepG2 hepatocytes did not proliferate well on the grafted PET scaffolds. Both cell-lines grew well on the nylon scaffolds.

Chapter 2: Hepatocyte proliferation and thermally induced cell detachment on 3D scaffolds

HC04 hepatocytes grown on Nylon-g-PNIPAAm-B matched the proliferation trend seen for the Algimatrix™ scaffold and, together with Nylon-cont, surpassed the Algimatrix™ proliferation when supporting HepG2 hepatocytes.

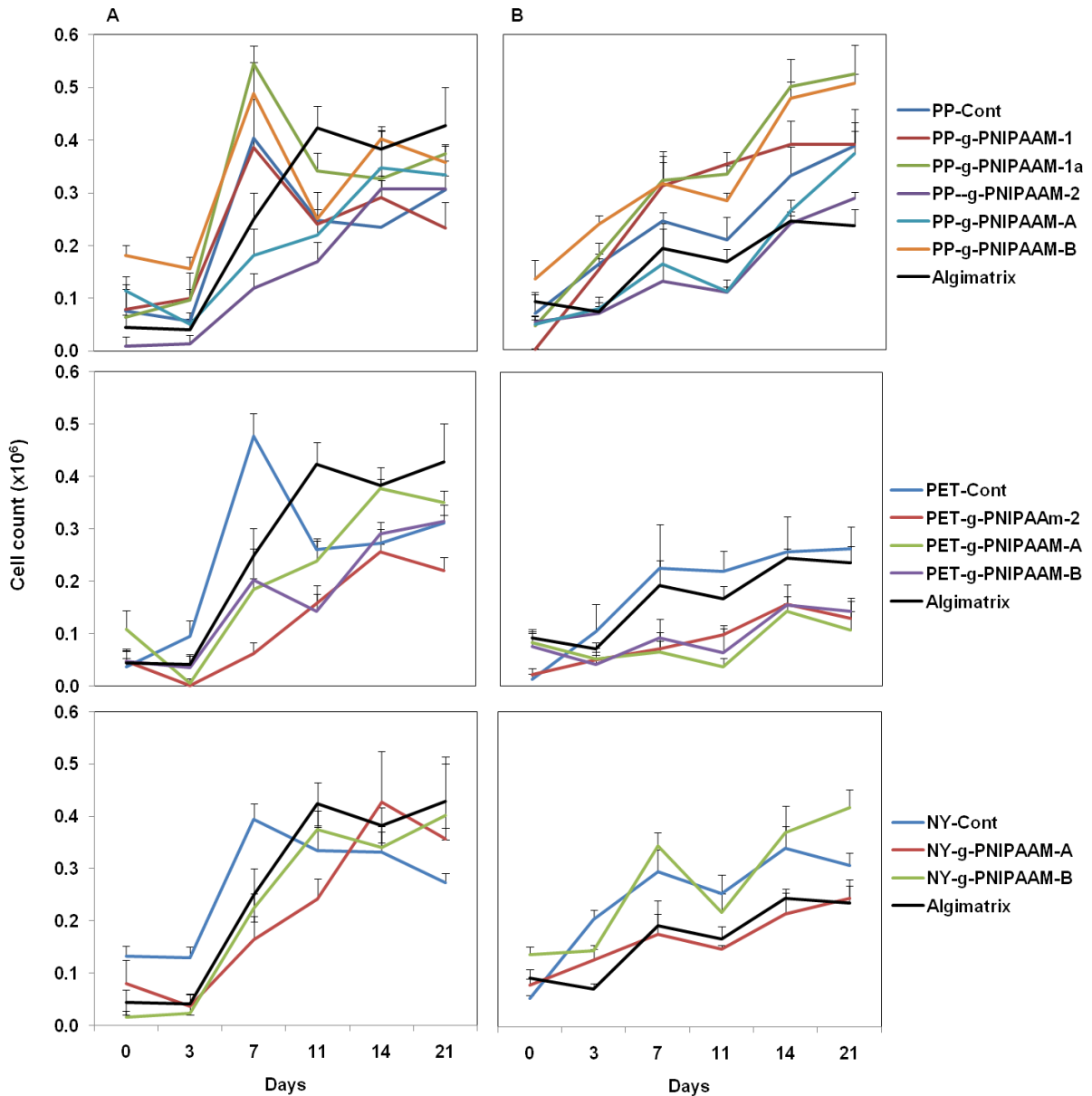


Figure 2.5. Cell proliferation on poly(propylene) (PP), poly(ethylene terephthalate) (PET) and nylon non-woven scaffolds, determined by the AB assay. HC04 (A) and HepG2 (B) hepatocyte cell-lines growing on different scaffolds as summarised in Table 2.2. were assayed for viability and proliferation using AB on 0 (hepatocyte retention in the scaffolds), 3, 7, 11, 14 and 21 dpi and are represented as number of cells. The data are presented as the average of five individual scaffolds \pm standard deviation.

Total DNA content of the cells was measured on 3, 7, 11, 14 and 21 dpi as an alternative means to measure cell proliferation on the 3D scaffolds; cell numbers were extrapolated from a standard curve generated for Hoechst 33258 (Figure 2.6).

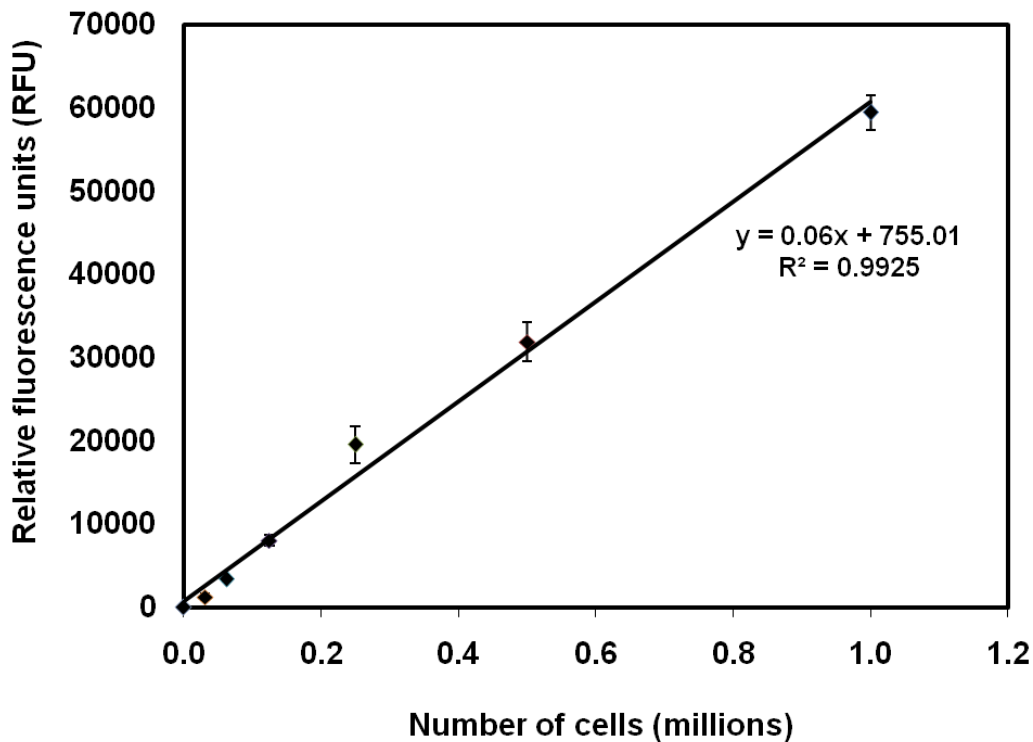


Figure 2.6. Hoechst 33258 standard curve using crude cell lysates as described by Rago *et al.* (118). A standard curve from crude cell lysates was generated from a predetermined number of hepatocytes (HC04 or HepG2) growing in a 24-well tissue culture plate with Hoechst 33258 at a final concentration of 10 $\mu\text{g}/\text{mL}$. The standard curve from HC04 hepatocytes is illustrated. The data are presented as the average of three replicates per cell number plotted against fluorescence \pm standard deviation.

Cell numbers derived from the DNA quantification results indicated that up to 5-fold more HC04 hepatocytes were growing on the scaffolds than suggested by the AB assay (Figure 2.6). The HC04 hepatocytes growing on the PP, PET and nylon scaffolds showed an approximate linear increase in numbers over time; however, there was not one scaffold that stood out as being far superior (or inferior) to the control scaffolds and AlgimatrixTM. Overall, DNA quantification-derived cell numbers of the HepG2 hepatocytes on the scaffolds more closely resembled the trend observed in the AB assay. As with the HC04 cells, no difference in growth on the grafted scaffolds as compared to the control scaffolds and AlgimatrixTM was observed (Figure 2.7). A general decrease in HepG2 DNA levels was seen on day 11 on the PET and nylon scaffolds and on day 14 on the PP scaffolds after which DNA levels recovered or remained relatively constant.

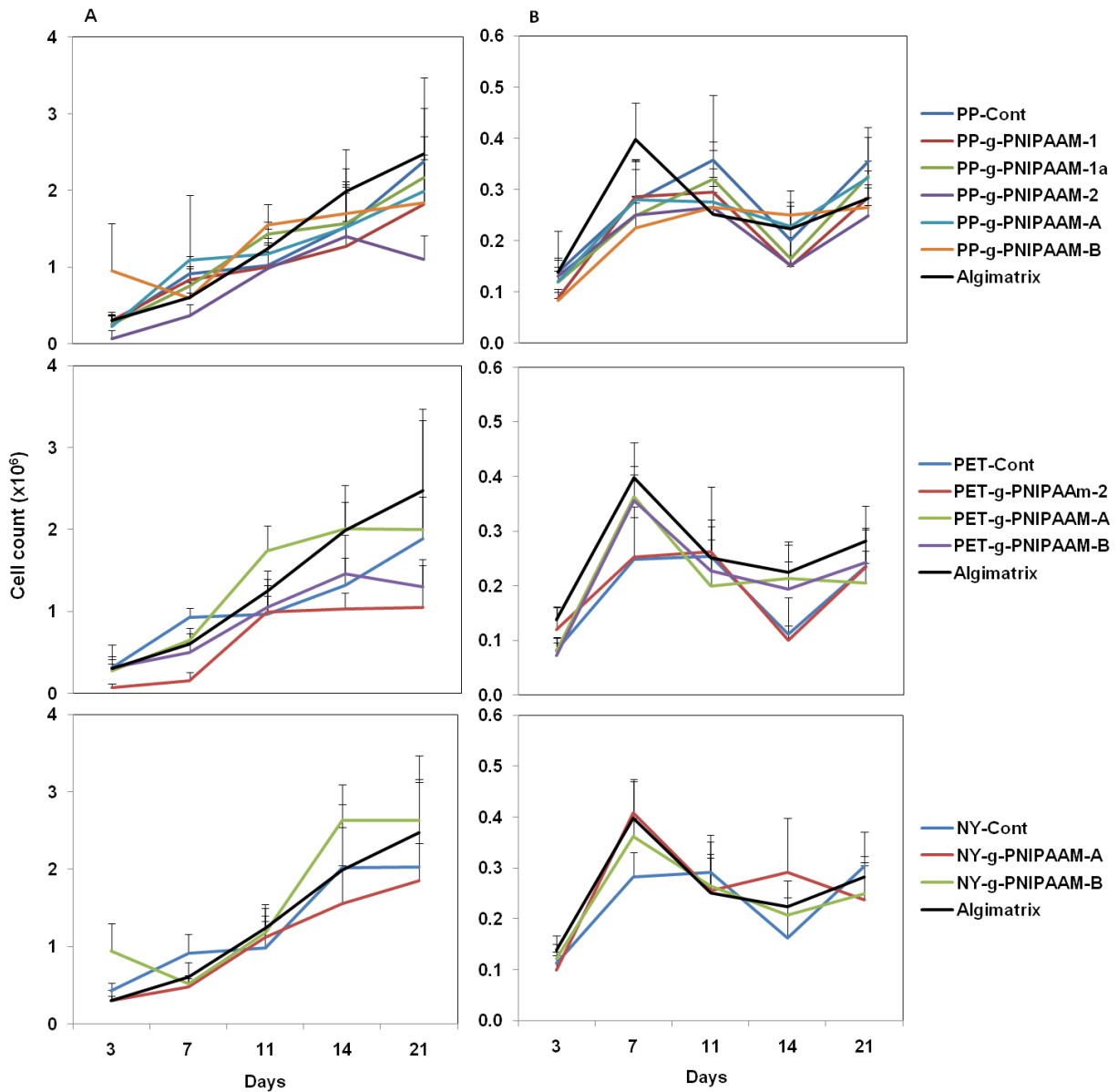


Figure 2.7. Cell proliferation of hepatocytes growing on poly(propylene) (PP), poly(ethylene terephthalate) (PET) and nylon non-woven scaffolds, determined by DNA staining. The proliferation of HC04 (A) and HepG2 (B) hepatocyte cell-lines growing on different scaffolds (as summarised in Table 2.2) was calculated using Hoechst 33258 fluorescence on 3, 7, 11, 14 and 21 dpi. The data are presented as the average of five individual scaffolds \pm standard deviation.

2.3.3. Fluorescence microscopy and albumin quantification

As an indicator of cell viability and functionality, fluorescence microscopy and albumin production was used to determine cell morphology and metabolic activity. Representative cell morphology and proliferation of the HC04 and HepG2 hepatocytes on the PP-g-PNIPAAm-B scaffold over 21 days is shown in Figure 2.8. HC04 hepatocytes grow along the non-woven fibres and at later time points form large cell clusters whereas the HepG2 hepatocytes have a greater tendency to form spheroids soon after seeding. The large cell clusters and spheroids

Chapter 2: Hepatocyte proliferation and thermally induced cell detachment on 3D scaffolds

are a desirable morphology for certain 3D cell culture applications as spheroids are highly metabolically active and physiologically representative cell formations.

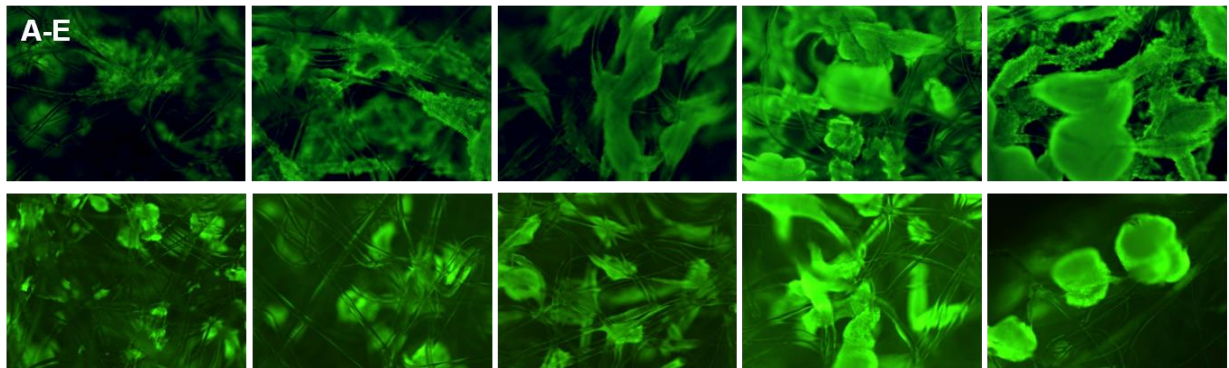


Figure 2.8. Representative fluorescence micrographs of HC04 (top panel) and HepG2 (bottom panel) hepatocytes growing on the PP-*g*-PNIPAAm-B scaffold after 3, 7, 11, 14 and 21 dpi (A-E). Cells were stained with Fluorescein Diacetate (FDA) and visualisation was performed at 40x magnification using a standard fluorescence microscope (Olympus BX41) equipped with a 490 nm bandpass filter with a 510 nm cut-off filter for fluorescence emission.

Hepatocyte metabolic activity was measured by quantifying albumin production (indicating active protein biosynthesis) of hepatocytes grown on pure PP scaffolds (mean pore size of 200 μm). Albumin production in 2D and 3D cultures was quantified on 3, 5, 7, 10, 14 and 21 dpi and normalised to total protein. Fluorescent values obtained in each assay were plotted against their respective standard curves (Figure 2.9) and the data were expressed as expression fold change as compared to the 2D values.

Chapter 2: Hepatocyte proliferation and thermally induced cell detachment on 3D scaffolds

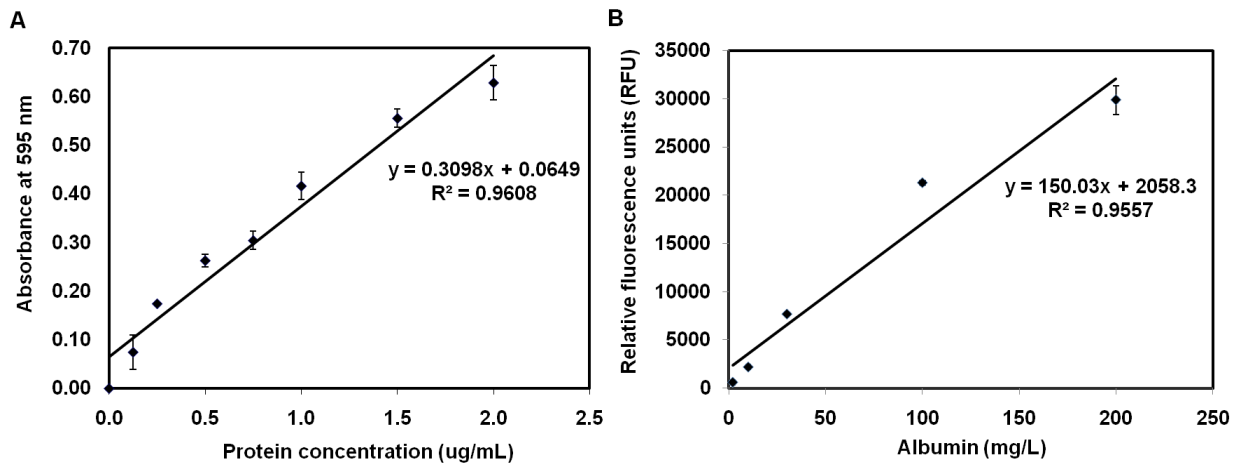


Figure 2.9. Bradford assay and albumin standard curves. **A.** The Bradford standard curve was performed as a 250 μ L microplate assay using the bovine gamma-globulin standard set with seven concentrations of gamma globulin: 2, 1.5, 1, 1.75, 0.5, 0.25 and 0.125 μ g/mL. The data are presented as the average of three replicates per concentration plotted against absorbance at 595 nm \pm standard deviation. **B.** The albumin standard curve was generated using the calibrator solution in the Albumine Fluorescence Assay Kit (Sigma-Aldrich). The albumin stock solution was diluted to final concentrations of 2, 10, 30, 100 and 200 mg/mL and the fluorescence was read at excitation and emission wavelengths of 600 and 630 nm respectively. The data are presented as the average of three replicates per concentration plotted against fluorescence \pm standard deviation.

Albumin production of hepatocytes cultured in 3D was compared to albumin production in hepatocytes cultured in 2D.

HC04 hepatocytes secreted, on average, twice the amount of albumin when cultured on the 3D PP non-grafted scaffolds as compared to the 2D monolayer, indicating that cells growing in the 3D context were more metabolically active than their 2D counterparts (Figure 2.10). In contrast, the HepG2 cells took longer to exceed the levels of albumin secreted by the 2D monolayer, achieving a maximum 1.5-fold increase at 21 dpi.

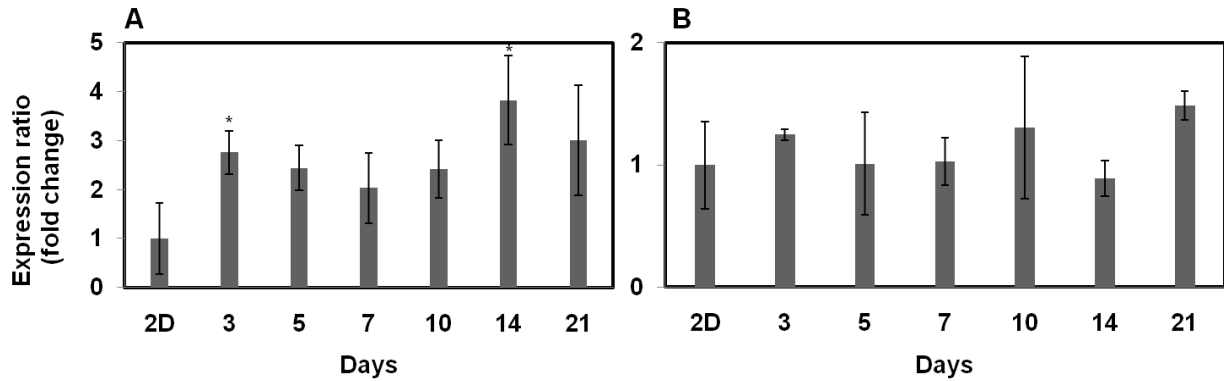


Figure 2.10. Relative albumin secretion in HC04 (A) and HepG2 (B) hepatocytes growing on a 3D non-woven control scaffold (pore size 200 μm). Known quantities of human albumin were used to establish a calibration curve and the quantities of albumin secreted into culture media were normalised to total protein levels in the media as determined by the Bradford assay to correct for differences in cell numbers. The data are indicated as fold change of cells growing in 3D compared to cells grown as a 2D monolayer. Data are the average of three individual scaffolds \pm standard deviations; * indicates significance at $P < 0.05$ (student T-test).

2.3.4. Cytochrome P450 mRNA expression

CYP gene expression was monitored using qRT-PCR in HC04 cells grown on PP-Cont non-woven scaffolds modified to have a mean pore size of 200 μm (Figure 2.11 A) and compared to the CYP gene expression in hepatocytes growing in 2D in order to compare cell metabolic function. CYP genes code for enzymes that are involved in the oxidation of organic compounds to enhance excretion and play a major role in the metabolism of drugs and xenobiotics. It has been hypothesised that hepatocytes growing in 3D may display enhanced drug metabolism due to higher levels of endogenous CYP gene expression.

Primers designed for CYP gene expression analysis are listed in Table 2.3. The expression of these genes was normalised against that of β -actin as housekeeping gene. Primers were designed using Primer3 (124).

Table 2.3. Primer sequences for cytochrome qRT-PCR.

Gene	Accession number	Forward primer (5'→3')	Reverse Primer (5'→3')	Product length (bp)
CYP2C19	NM_000769.1	TGCACGAGGTCCAGAGATACAT	TTTAACGTCACAGGTCACCTGCAT	71
CYP2C9	NM_000771.3	CCTGACTTCTGTGCTACATGACAA	ATTGCCACCTTCATCCAGAAA	85
CYP1A2	NM_000761.3	CTCCTCCTTCTTGCCCTTCA	GTTTACGAAGACACAGCATTTCTTG	97
CYP2D6	NM_001025161.1	TGTGCCCATCACCCAGATC	TCACGTTGCTCACGGCTTT	95
CYP3A4	NM_017460.3	GCAAGAAGAACAAGGACAACATAGAT	GCAAACCTCATGCCAATGC	85
CYP3A5	NM_000777.2	TGGGACCCGTACACATGGA	GACAAAACATTTCCAACAAAGG	81
β -actin	NNM_001101	CCTGGCACCCAGCACAAT	GCCGATCCACACGGAGTACT	70

Chapter 2: Hepatocyte proliferation and thermally induced cell detachment on 3D scaffolds

Expression levels of *CYP2C9*, *2C19*, *3A4* and *3A5* increased over time as the 3D scaffold became more densely populated, with *CYP1A2*, *2C19* and *3A5*, up-regulated compared to the 2D control. *CYP2C19* for example, was expressed 79-times higher (significance $P < 0.05$) in the cells growing on the scaffold compared to the 2D control, using β -actin as the internal qRT-PCR reference control for cell numbers. For two genes, namely *CYP2C9* and *3A4*, levels of gene expression remained equal to, or below, that seen for HC04 cells grown in 2D. This experiment revealed the highest level of CYP expression to be at 21 dpi (Figure 2.11 A). On this basis, similar quantification of the selected CYP genes was performed at 21 dpi using HepG2 hepatocytes grown on the scaffolds.

qRT-PCR revealed that CYP genes *1A2*, *2C9* and *2C19* were up-regulated at day 21 while the expression levels of CYP genes *3A4* and *3A5* were less than that of the 2D control. *CYP2D6* was expressed at a similar level to that of the 2D control (Figure 2.11 B). When the CYP gene expression levels were assessed on scaffolds of different mean pore size that had been grafted (using grafting method of scaffold PP-*g*-PNIPAAm-B) it was noted that gene expression was increased for all the selected genes as depicted in Figure 2.11 C. No specific conclusion can be drawn as to which pore size performed the best; however, the scaffolds PP-*g*-PNIPAAm-B1 (100 μm mean pore size) and PP-*g*-PNIPAAm-B2 (150 μm mean pore size) appeared to support higher levels of gene expression than PP-*g*-PNIPAAm-B3 (200 μm mean pore size).

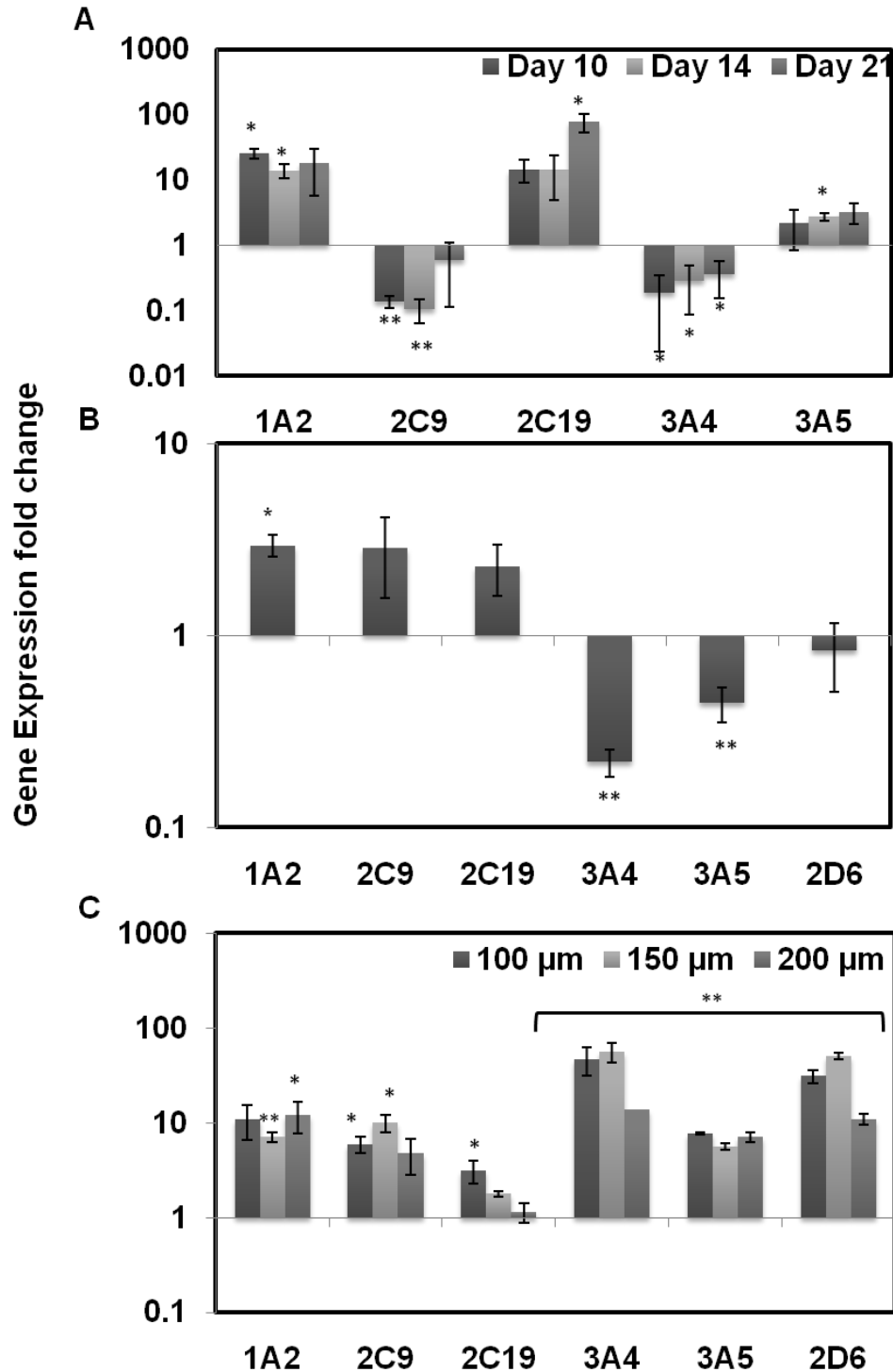


Figure 2.11: CYP gene expression of 3D hepatocytes relative to 2D hepatocytes. **A.** HC04 hepatocyte CYP gene expression after 10, 14 and 21 days of growth on the non-grafted, 200 μm pore size, poly(propylene) (PP) scaffolds. **B.** HepG2 cytochrome gene expression after 21 days of growth on the same PP non-woven scaffolds as described for graph A. **C.** HC04 cytochrome gene expression after 21 days of growth on scaffolds PP-g-PNIPAAm-B1 (100 μm), PP-g-PNIPAAm-B2 (150 μm) and PP-g-PNIPAAm-B3 (200 μm). Expression of each transcript, relative to a 2D HC04 monolayer culture, was determined using the $2^{-\Delta\Delta C_t}$ method by normalising to β -actin expression and is graphed as fold induction compared to 2D. Data are represented as the average of three independent experiments performed in triplicate \pm standard deviations. * indicates significance at $P < 0.05$ and ** indicates significance at $P < 0.01$ (student T-test).

2.3.5. Thermal release

An initial thermal release trial was conducted to ascertain which non-woven polymer, grafting and sterilisation method (autoclaving or ethanol) permits optimal cell release at 20°C using HC04 hepatocytes that had grown on the scaffolds for 10 dpi. Thermal release of HC04 hepatocytes at 20°C was observed most significantly after 2 h on the PP-*g*-PNIPAAm-A and PP-*g*-PNIPAAm-B scaffolds that had been ethanol sterilised (Figure 2.12). No other scaffold displayed significant thermal cell release. Although some scaffolds did appear to release cells, including PET-*g*-PNIPAAm-A (autoclaved, 1 h release), PET-*g*-PNIPAAm-B (ethanol, 2 h release) and Nylon-*g*-PNIPAAm-A (autoclaved, 2 h release), these scaffolds were also observed to drop non-woven fibres, ruling out the possibility that thermal release alone was responsible for the released cells. This result was subsequently confirmed using HC04 and HepG2 cells (Figure 2.13).

Chapter 2: Hepatocyte proliferation and thermally induced cell detachment on 3D scaffolds

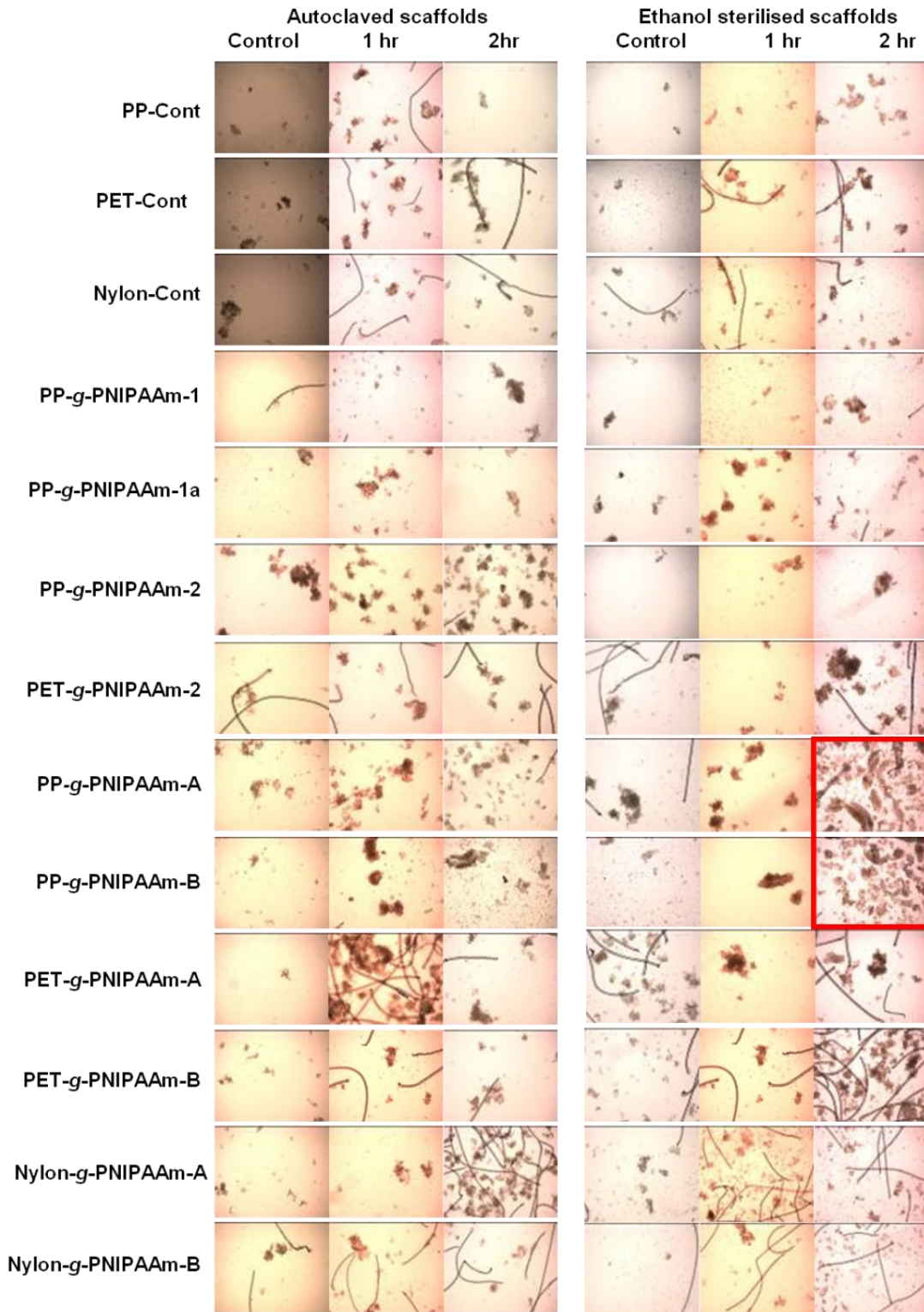


Figure 2.12. Thermal release of HC04 hepatocytes from grafted and control scaffolds 10 dpi. Autoclaved and ethanol sterilised scaffolds were allowed to incubate at 37°C (control) and 20°C for 1 h and 2 h to assess the potential of each scaffold to undergo temperature induced cell release. The red box around PP-g-PNIPAAm-A and PP-g-PNIAPPM-B (both ethanol sterilised) after 2 h at 20°C indicates successful thermal release of the cells from the scaffolds based on a visual comparison as compared to their respective controls which were maintained at 37°C. Images of the dropped cells were taken using bright-field illumination and a 4x objective on a standard microscope (Olympus BX41).

Chapter 2: Hepatocyte proliferation and thermally induced cell detachment on 3D scaffolds

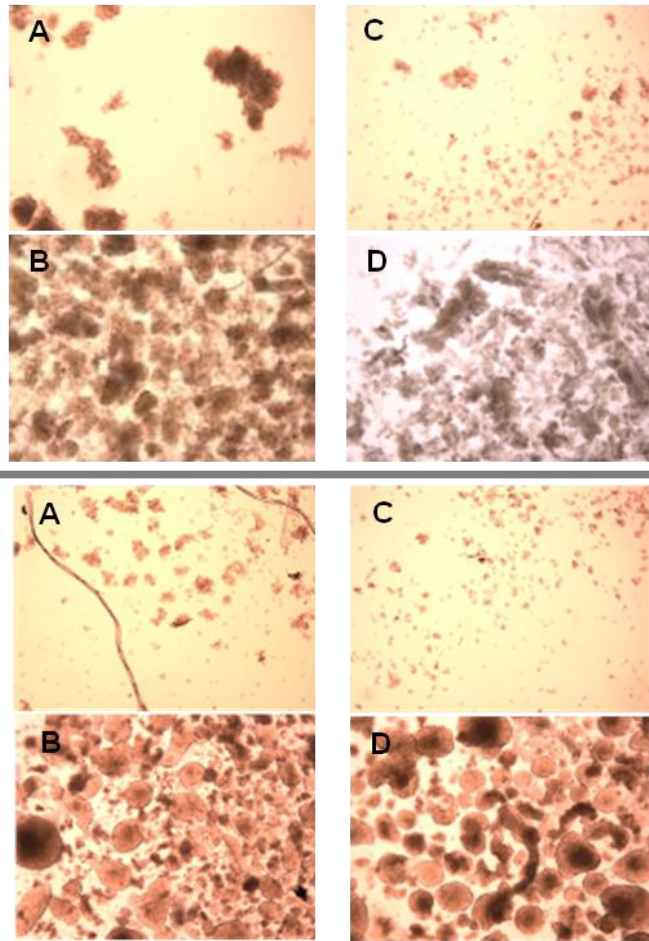


Figure 2.13. Thermal release of HC04 and HepG2 hepatocytes. Cells were grown on either PP-*g*-PNIPAAm-A (left hand panels) or PP-*g*-PNIPAAm-B scaffolds (right hand panels) for 10 days. Cell release was compared between scaffolds kept at 37 °C (A, C) or at 20°C (B, D) for 2 h for both HC04 (top panels, A-D) and HepG2 cells (bottom panels, A-D). Images of cells dropped from the scaffolds were taken using a standard microscope (Olympus BX41) at 40x magnification.

Additional controls were included to verify that none of the other components of the grafting process other than the presence of PNIPAAm was responsible for the observed cell release. Scaffold PP-*g*-PNIPAAm-B which had been oxyfluorinated and grafted displayed greater capacity for thermal release than the “test 2” and “test 4” scaffolds (Table 2.1), which had not been grafted with PNIPAAm. In addition scaffold PP-*g*-PNIPAAm-B released more cells than scaffold “test 3” which had been grafted but had no prior surface functionalisation i.e. oxyfluorination (Figure 2.14).

Chapter 2: Hepatocyte proliferation and thermally induced cell detachment on 3D scaffolds

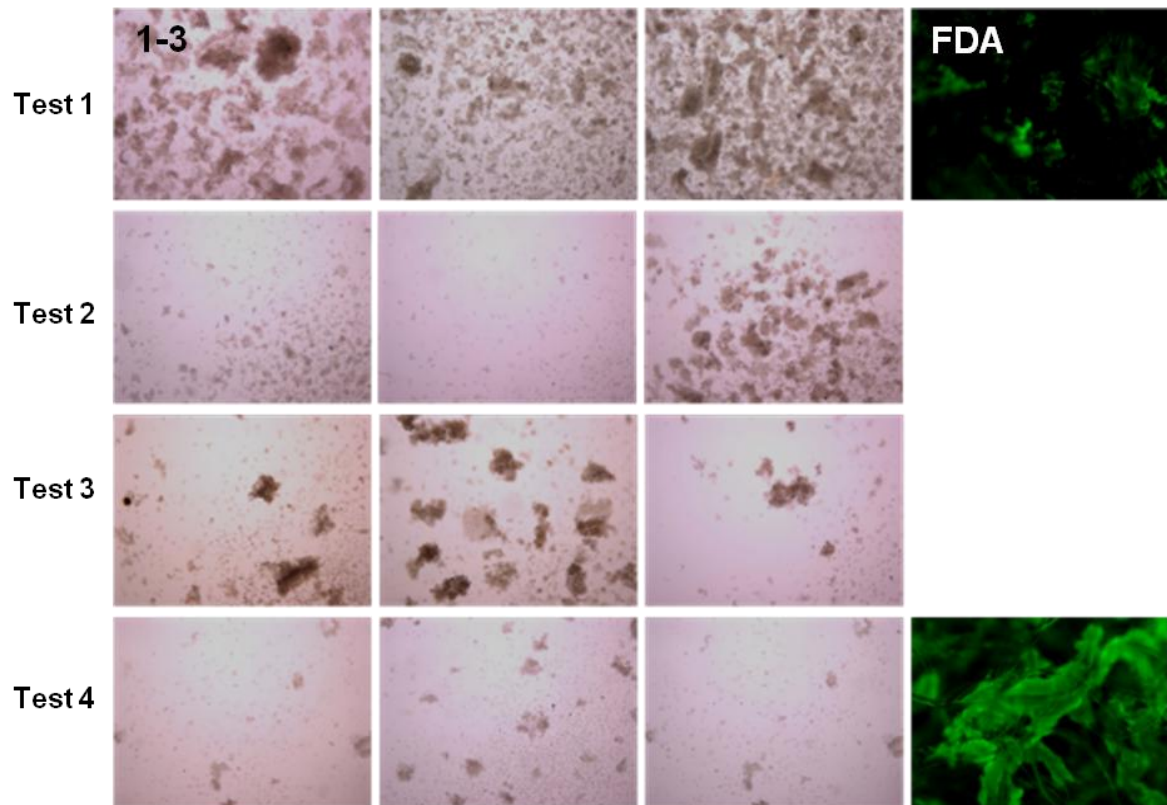


Figure 2.14. Additional controls used to assess if omitting any stages of the grafting process have any effect on thermal release. Panels 1-3 are HC04 hepatocytes dropped from biological replications of each of the grafting variations, Test 1 – Test 4 as summarised by Table 2.2. Thermal release of cells that had been growing on ethanol sterilised scaffolds (Test 1-4) for 10 days took place at 20°C for 2 h. Thermal release images of the dropped cells were taken using a standard microscope (Olympus BX41) with a 4x objective. HC04 hepatocytes remaining on the scaffolds Test 1 (grafted) and Test 4 (not grafted) after thermal release were visualised using fluorescein diacetate (FDA, Sigma) at 40x magnification using an Olympus BX41 microscope equipped with a 490 nm bandpass filter with a 510 nm cut-off filter for fluorescence emission.

It can thus be concluded that only the addition of PNIPAAm during the grafting procedure will result in release of cells from the scaffolds when the temperature is lowered below the LCST and that no other exogenous factors contribute to the observed cell release. In addition to this, grafted scaffolds with different pore sizes were tested to see if this had any effect on thermal release of the cells; after 10 days in culture it was observed that pore size does not significantly affect cell release from the scaffolds with mean pore sizes of 100, 150 or 200 μm , based on visual estimation (Figure 2.15).

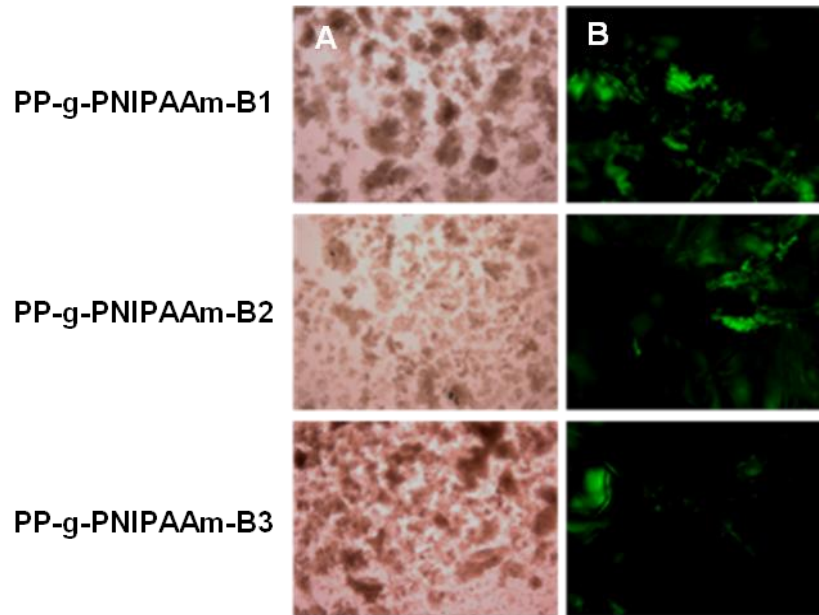


Figure 2.15. Effect of non-woven scaffolds' pore size on thermal release. HC04 hepatocytes were released after 10 days of growth from ethanol sterilised scaffolds: PP-*g*-PNIPAAm-B1 (mean pore size 100 μm) PP-*g*-PNIPAAm-B2 (mean pore size 150 μm) and PP-*g*-PNIPAAm-B3 (mean pore size 200 μm) as summarised in Table 2.2 at 20°C for 2 h. Images of the dropped cells were taken using a standard microscope (Olympus BX41) at 40x magnification. Fluorescent images of the cells remaining on the scaffolds after thermal release were taken using fluorescein diacetate (FDA, Sigma) using an Olympus BX41 microscope equipped with a 490 nm bandpass filter with a 510 nm cut-off filter for fluorescence emission.

A quantitative estimation of cell recovery rates from the scaffolds was also conducted. Scaffolds PP-*g*-PNIPAAm-B1, PP-*g*-PNIPAAm-B2 and PP-*g*-PNIPAAm-B3 were seeded with HC04 hepatocytes. At 14 dpi, the number of total cells on the scaffolds was estimated using the AB assay. Trypsin treatment of the scaffolds or thermal release was used to remove cells from the scaffolds ($n=3$). Viable cells released from the scaffolds were counted using trypan blue dye exclusion. Trypsin treatment of scaffolds PP-*g*-PNIPAAm-B1 and PP-*g*-PNIPAAm-B2 yielded approximately as many cells as the thermal release, however, more viable cells were released from PP-*g*-PNIPAAm-B3 after trypsin treatment than thermal release. In all instances with the exception of scaffold PP-*g*-PNIPAAm-B3 treated with trypsin (Table 2.4), fewer cells were released than the total estimated to be growing on the scaffold using AB thus indicating that neither trypsin nor thermal release is fully effective in releasing all the cells.

Table 2.4. Hepatocyte cell release from scaffolds PP-g-PNIPAAm-B1, PP-g-PNIPAAm-B2 and PP-g-PNIPAAm-B3 via trypsin treatment or thermal release. Total hepatocyte numbers on the scaffolds prior to cell release were estimated using AB. Viable cells released from the scaffolds were counted using trypan blue dye exclusion on a haemocytometer. The data are presented as the average of three individual scaffolds.

	PP-g-PNIPAAm-B1	PP-g-PNIPAAm-B2	PP-g-PNIPAAm-B3
Total Cells	556 206	608 985	468 552
Trypsin	270 000	190 000	530 000
Thermal Release	230 000	230 000	250 000

Viable cells released from the scaffolds were seeded into a 6 well plate and re-attachment and growth was observed as an additional indication of viability post release (data not shown).

2.3.6. Automated cell culture device

The automated system was designed such that a final (potentially commercial) system would contain a permanent base unit containing the re-usable hardware fitted with a single-use set of consumable components, which would be pre-packed and sterilised. The system hardware would be a once-off acquisition that would be re-used for consecutive cell culturing experiments and would include the perfusion pump, heating/cooling equipment, valves and the permanent base unit (the platform upon which the tubing and bioreactor will be mounted). The consumable set would contain the “wetted” perfusion components including all the perfusion tubing, pinch valve segments, sampling ports, T-sections, etc; the media reservoirs; the bioreactor unit; the oxygenator unit; instrumentation probes that are in direct contact with the perfusion media (oxygen probes, etc.); and the gas supply sterility filters.

Functioning of the automated system will involve circulation of cell culture medium from the medium reservoir to the bioreactor which will contain the non-woven scaffolds; cells are then seeded into the bioreactor; sufficient time is allowed for the bioreactor to be populated with cells and then cell release is affected by lowering the temperature of the cell culture medium to detach cells from the scaffolds grafted with PNIPAAm. The medium containing cells would then be recovered and centrifuged separately for cell separation from the media; this process is illustrated in Figure 2.16. For the purposes of our study the entire automated cell culture device was placed into an incubator set at 37°C to regulate the temperature.

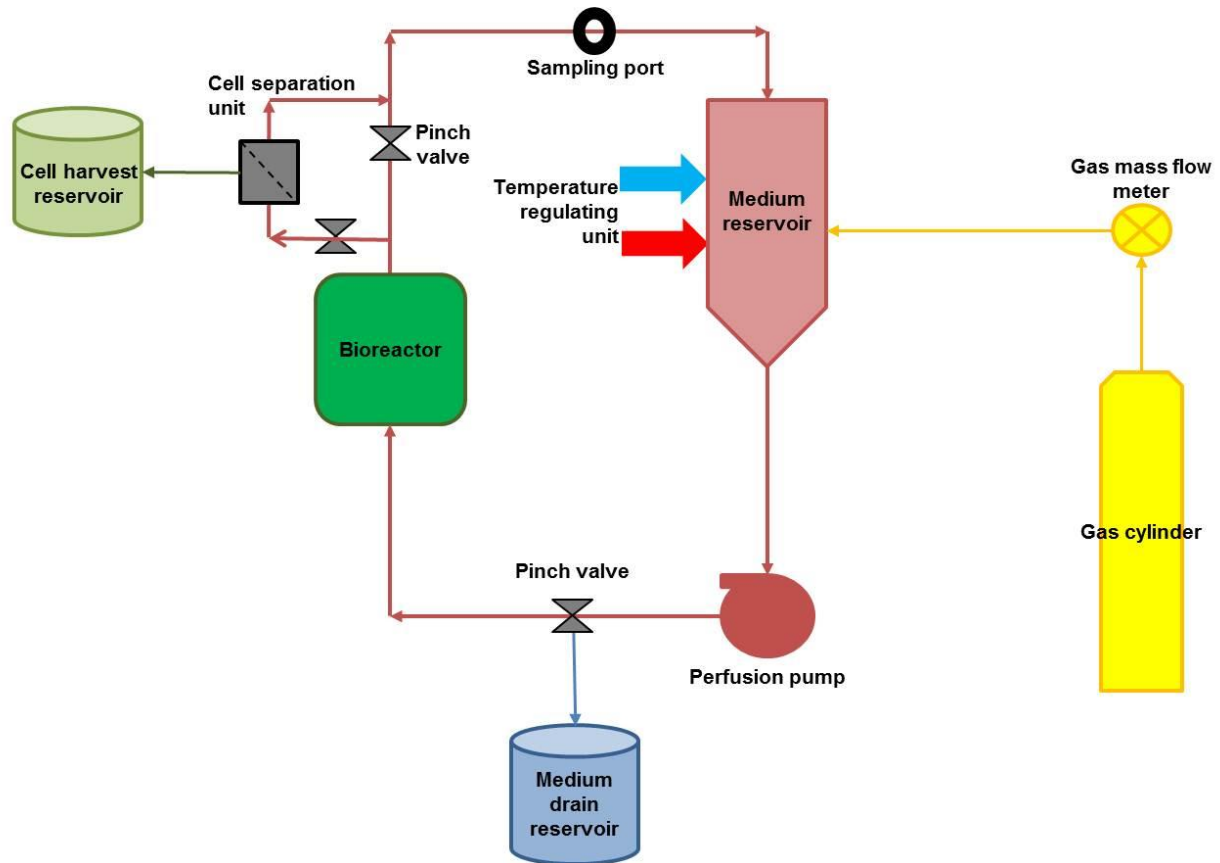


Figure 2.16. The perfusion circuit layout and system components of the proposed automated cell culture system (Figure courtesy of AJ van Wyk, Blueline Designs, re-drawn by C. Rossouw).

2.3.6.1. Prototype

PP un-grafted scaffolds (mean pore size of 200 μm) were punched into disks (15 mm in diameter and 3 mm thick). Three scaffolds were used in the bioreactor per experiment, which was pre-cultured overnight (pump speed 5 mL/min) to remove any debris and to ascertain whether the bioreactor and scaffolds had been adequately sterilised. The overnight media was replaced with fresh, warm media (37°C). The data for the different seeding methods using HC04 hepatocytes are presented in Table 2.5. By seeding the hepatocytes directly into the bioreactor and allowing them to attach over a period of 2-3 h most of the hepatocytes were retained in the bioreactor. In addition, an experiment was conducted when the bioreactor was run over a period of 7-10 dpi to ascertain that if the cells were not growing well on the scaffolds, where within the automated system they were becoming trapped. Once the automated system was stopped the media was drained and the scaffolds with cells attached gently removed from the bioreactor. The scaffolds, medium reservoir, bioreactor and tubing were trypsinised and the cells were harvested and counted by trypan blue dye exclusion on a haemocytometer.

Chapter 2: Hepatocyte proliferation and thermally induced cell detachment on 3D scaffolds

Table 2.5. Experimental parameters assessed using the prototype automated cell culture device

Bioreactor Seeding Method				
Delivery Into media reservoir	Pump Speed	Media flow direction	Viable cells in media after 3 h	
Media static				
2x10 ⁶	2 mL min ⁻¹	Up into bioreactor		24 000
2x10 ⁶	2 mL min ⁻¹	Up into bioreactor		16 000
Media stirred				
4.5x10 ⁶	2 mL min ⁻¹	Up into bioreactor		64 000
4.x10 ⁶	2 mL min ⁻¹	Up into bioreactor		69 000
Into bioreactor				
4.5 x 10 ⁶	Static	Up into bioreactor		27 000
4.5 x 10 ⁶	Static	Up into bioreactor		12 000
Cell proliferation				
Trial 1				
Number of cells seeded	Pump Speed	Media flow direction	Days in culture	Number of viable cells
4.5 x 10 ⁶ (into bioreactor)	0.5 mL min ⁻¹	Up into bioreactor	7	Media reservoir 0 Bioreactor glass 60x10 ⁴ Within tubing 5x10 ⁶ Non-woven scaffolds 8x10 ⁶ Total: 13.6x 10⁶
Trial 2				
Number of cells seeded	Pump Speed	Media flow direction	Days in culture	Number of viable cells
4.5 x 10 ⁶ (into bioreactor)	0.5 mL min ⁻¹	Up into bioreactor	7	Media reservoir 0 Bioreactor glass 1x10 ⁶ Within tubing 1.5x10 ⁶ Non-woven scaffolds 2.3x10 ⁶ Total: 4.8 x 10⁶
Trial 3				
Number of cells seeded	Pump Speed	Media flow direction	Days in culture	Number of viable cells
4.5 x 10 ⁶ (into bioreactor)	2 mL min ⁻¹	Down into bioreactor	10	Media reservoir 0 Bioreactor glass 0 Tubing 0 Non-woven scaffolds 49.9 x 10 ⁶ Total: 49.9 x 10⁶
Trial 4				
Number of cells seeded	Pump Speed	Media flow direction	Days in culture	Number of viable cells
4.5 x 10 ⁶ (into bioreactor)	2 mL min ⁻¹	Down into bioreactor	10	Media reservoir 0 Bioreactor glass 0 Tubing 0 Non-woven scaffolds 39.7 x 10 ⁶ Total: 39.7 x 10⁶

Chapter 2: Hepatocyte proliferation and thermally induced cell detachment on 3D scaffolds

By adjusting the direction of the media flow and its speed we observed up to a 10 fold increase in cell numbers over a 10 day period in trials 3 and 4.

An additional trial was conducted (trial 3 conditions, Table 2.5) in order to visually assess hepatocyte distribution between the scaffolds within the bioreactor. The scaffolds were removed from the bioreactor and stained with fluorescein diacetate as described in section 2.2.5. (Figure 2.17). Viable hepatocytes were observed to be attached to the scaffolds throughout the bioreactor.

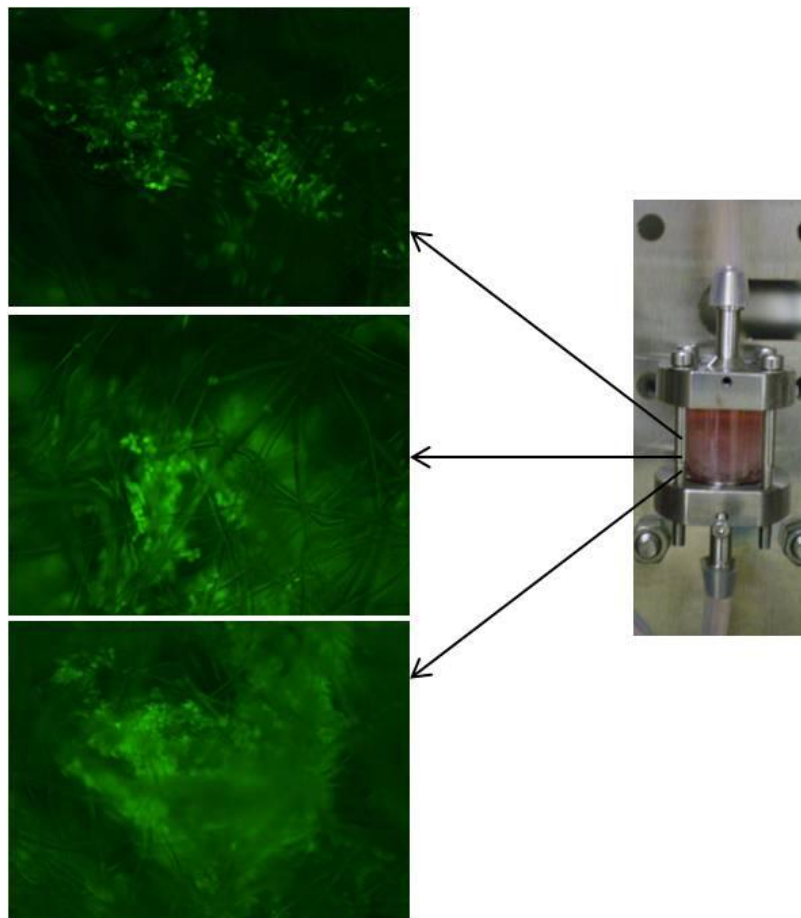


Figure 2.17. HC04 hepatocytes growing on the three non-woven scaffolds housed in the bioreactor. Fluorescent images of hepatocytes growing on the scaffold from the top, middle, and lower layers of the bioreactor 7 dpi. This illustrates that the seeding method enable cells to be distributed throughout the scaffolds in the bioreactor. The hepatocytes were stained with fluorescein diacetate (FDA, Sigma) and visualised at 40x magnification using an Olympus BX41 microscope equipped with a 490 nm bandpass filter with a 510 nm cut-off filter for fluorescence

2.3.6.2. Final system design and testing

During the initial cell culturing experiments on the final system, cells were seeded dynamically i.e. they were introduced in suspension in the medium reservoir and pumped through the bioreactor and scaffold. This seeding method resulted in cells adhering to all surfaces of the

Chapter 2: Hepatocyte proliferation and thermally induced cell detachment on 3D scaffolds

system and less on the non-woven scaffolds. During subsequent cell culturing experiments, the seeding procedure was optimized such that the cells were seeded statically above the bioreactor via a sampling port and allowed to settle via gravity onto the non-woven scaffolds in the bioreactor. The static conditions were maintained for 3 h before the bioreactor was perfused. The results obtained from this seeding methodology indicated much higher cell numbers attached to the scaffold, resulting in overall better performance of the cell culturing system. It was thus decided to adopt a gravity assisted, static seeding methodology in the final automated cell culture. Cells would be seeded from the sampling port located at the top of the bioreactor with perfusion of the system only commencing 3 h after seeding.

The initial cell culturing experiments revealed that the cells were adhering to the bottom of the medium reservoir as well as the inside lumen of the tubing. This was due to the gravitational settling of cells within the reservoir. Experimental manipulation by means of agitation of the medium reservoir using a magnetic stirrer resulted in fewer cells adhering to the bottom of the reservoir. In the final perfusion system design this aspect was addressed by designing the medium reservoir with an angled bottom medium intake that will allow any cells in suspension to settle towards the bottom of the reservoir from where they would be pumped back to the bioreactor i.e. media would flow out the bottom of the reservoir (Figure 2.18A). Once back in the bioreactor the cells would have the opportunity to adhere to the non-woven scaffold. Any anchorage dependant cell will tend to adhere to any available surface, this means that cells will adhere to the inside surface of the tubing and one of the best ways to limit the effect of cells adhering to the tubing is to reduce the length (i.e. surface area) of the tubing. In the final perfusion system design emphasis was placed on reducing the overall length of tubing of the system.

Air trapped in the prototype bioreactor resulted in uneven perfusion of the non-woven scaffolds. The entrapped air would accumulate below the scaffold on the outlet side of the bioreactor. Thus, the new design has incorporated a way in which to remove air bubbles forming below the scaffold as illustrated in Figure 2.18B and C. In addition this problem was somewhat overcome by perfusing the media down through the bioreactor as opposed to up through the bioreactor. The final automated system is photographed in Figure 2.18.

Chapter 2: Hepatocyte proliferation and thermally induced cell detachment on 3D scaffolds

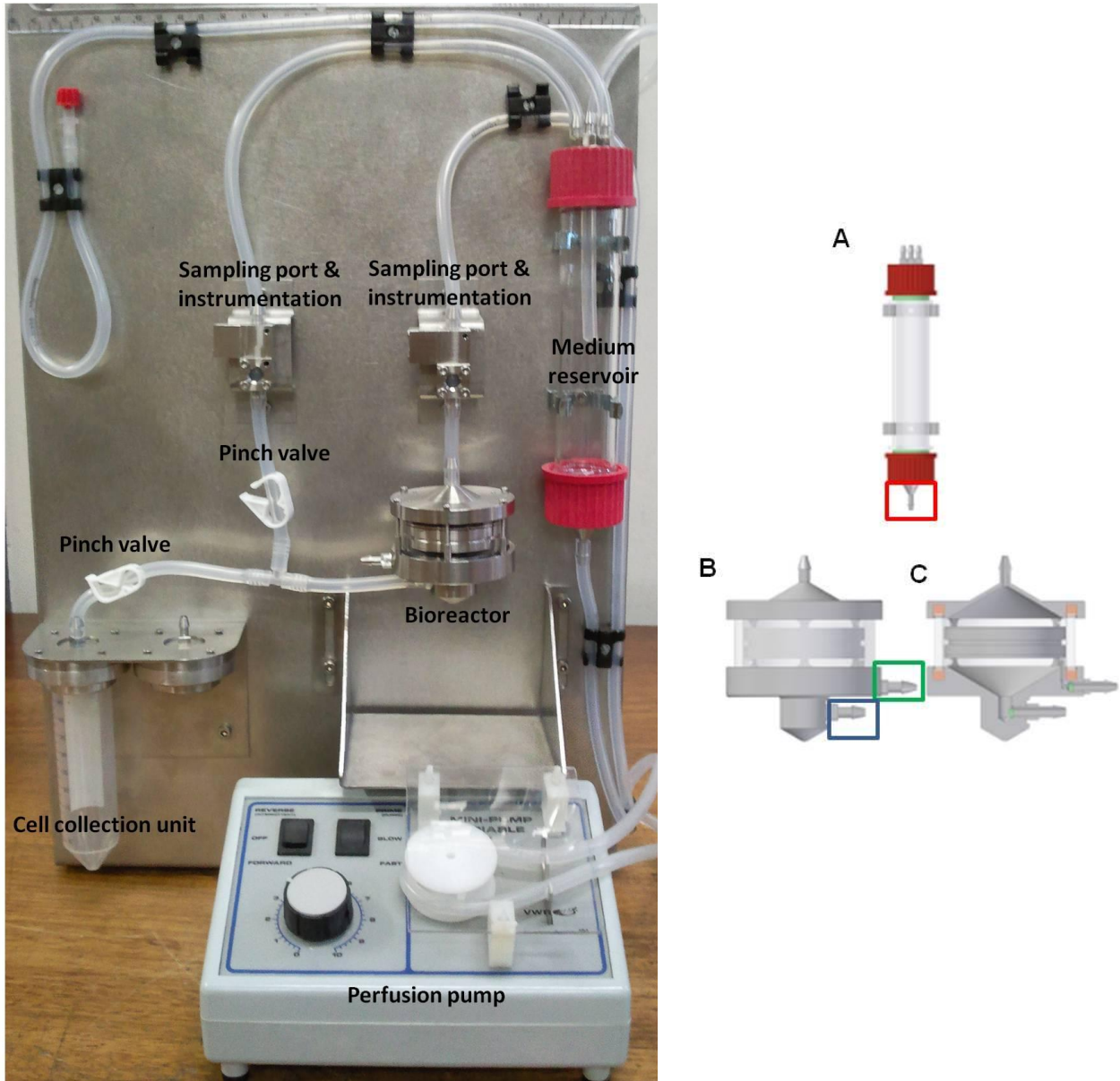


Figure 2.18. The final automated cell culture system. The new automated system is photographed on the left. **A.** The new medium reservoir. Media is pumped out of the bottom of the reservoir (red box) thus preventing cells settling on the bottom of the reservoir and eliminating the need to stir the media. **B.** The new bioreactor with medium outlet (blue box) and air bubble outlet (green box). **C.** A schematic cross section of the bioreactor.

The final automated system was tested using the parameters from trial 3 and 4 (Table 2.5), however, the pump speed was modified. In order to keep the bioreactor filled with media at all times the pump speed was set to 10 mL/min. Two million HC04 hepatocytes per non-woven scaffold (total 6 million) were seeded into the bioreactor via the sampling port and grown for 10 days. A control experiment using PP-Cont non-woven scaffolds (200 μm pores) was first performed. Thermal release was attempted by draining the warm (37°C) cell culture media and replacing it with media at room temperature (20°C). The media was perfused for 2 hours and the cell culture media containing any released hepatocytes was collected. Viable cells were counted using trypan blue dye exclusion and a haemocytometer. The non-woven scaffolds were

Chapter 2: Hepatocyte proliferation and thermally induced cell detachment on 3D scaffolds

then removed from the bioreactor and the cells remaining on the non-woven scaffolds trypsinised as in section 2.2.3 and collected. Viable hepatocytes were counted using trypan blue dye exclusion and a haemocytometer. This experiment was repeated using PP-g-PNIAPPA-B1 non-woven scaffolds. The data are presented in Figure 2.19.

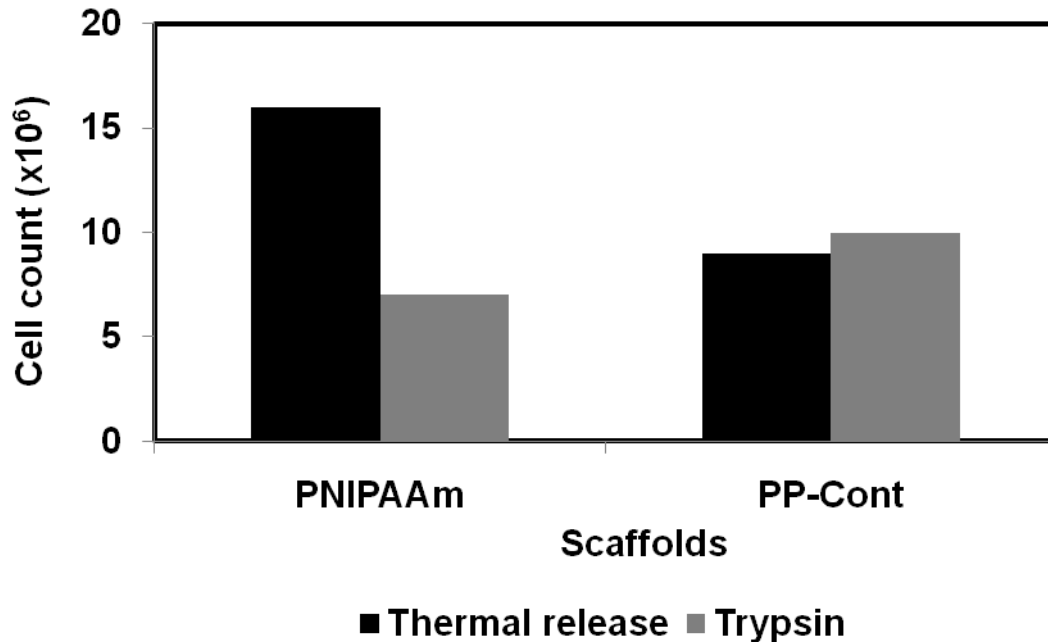


Figure 2.19. HC04 hepatocytes released from grafted (PP-g-PNIPAAm-B1) and control (PP-Cont) non-woven scaffolds 10 dpi in the final automated system. Approximately 16 million cells were released by the grafted non-woven scaffold after temperature reduction and a further 7 million were released from the non-woven scaffolds after trypsination. Nine million hepatocytes were released from the control non-woven scaffolds after the temperature reduction and a further 10 million after trypsination.

The data indicate that, of the cells released, just under 50% (9 million) of the hepatocytes growing on the control scaffolds are released when the temperature of the circulating cell culture media is dropped and the rest of the cells (10 million) are subsequently released via trypsin on the control scaffolds. Approximately 16 million hepatocytes were released from the grafted scaffolds (PP-g-PNIPAAm-B1) and less than half that number (7 million) remained on the scaffolds when the balance of the cells was released via trypsin were counted. This experiment was not repeated due to the limited number of grafted scaffolds available so reproducibility of this experiment was not assessed. These preliminary data do however, support the hypothesis that cells can proliferate in the bioreactor and be released by reduction of temperature.

2.4. DISCUSSION

A growing body of evidence has emerged where cells grown *in vitro* in 3D structures have been shown to be significantly different and more representative of the physiological state of the native source tissue than those grown in conventional 2D monolayer cultures. The development of new culturing systems that enhance this capability is therefore expected to lead to significant advances in the predictive accuracy of multiple *in vitro* cell culture applications, including the fundamental study of cell growth and signalling, host-pathogen interactions, and the drug discovery process. In this study, the need was identified to develop a scaffold which could not only support cell attachment and enhanced proliferation, but could furthermore be capable of releasing 3D cell structures non-invasively for downstream applications. This is the first report for the development of 3D, thermoresponsive, non-woven scaffolds able to release cells from a 3D matrix without the use of enzymatic detachment or degradation of the scaffold. The feasibility of using three different polymers for enhanced 3D cell culture, grafted by various means with PNIPAAm, was investigated.

AB (non-destructive assay) and Hoechst 33258 (destructive assay) were used independently for determining the number of viable cells growing on the non-woven scaffolds as, to date, there is not one wholly accepted method for cell enumeration in 3D (125). For the majority of scaffolds tested using the AB assay, cell numbers, for both HC04 and HepG2 hepatocytes, were observed to initially increase after seeding but subsequently declined between days 7 and 11; thereafter cell numbers recovered and increased. Similar results have previously been observed by Shor *et al.* (115) in the interaction of osteoblasts with PCL / hydroxyapatite scaffolds. It has been suggested that this observed trend is due to the inability of the dye to penetrate the scaffolds and react with the cells in the interior of the scaffolds. The recovery in cell numbers can be attributed to cells subsequently populating areas of the scaffold where the dye can more easily penetrate. The cell numbers estimated using the AB assay will not be accurately representative of the inner construct environment if a metabolite concentration gradient existed between the interior and the exterior of the construct and is therefore dependent on the efficiency of metabolite diffusion into and out of the construct. This can be overcome to a degree by swirling the wells containing the scaffolds during the incubation period to assist dye diffusion, however, this diffusivity of reagents into the 3D environment can ultimately become a confounding factor in this type of assay and it is thus important to use AB in combination with another cell quantification assay. The AB assay did, however, reveal that the cells were able to proliferate on the grafted scaffolds at a level comparable to, and in some instances better than

Chapter 2: Hepatocyte proliferation and thermally induced cell detachment on 3D scaffolds

that of the commercially available alginate scaffold, Algimatrix™ and the control scaffolds, suggesting an absence of scaffold-induced cytotoxicity.

The Hoechst 33258 assay indicated that the HC04 cells proliferated rapidly on the scaffolds whereas the growth of the HepG2 hepatocytes was relatively static over time. This can be largely attributed to the different way in which these cells grow. Fluorescence microscopy revealed that the HC04's displayed guided growth according to the non-woven fibre orientation forming 3D structures as depicted in Figure 2.9 and populating the majority of the scaffold surface area. HepG2 cells formed spheroids with a small area of attachment to the non-woven fibres soon after seeding into the scaffolds thus they did not populate the scaffolds as rapidly or as extensively as the HC04 cells. This discrepancy in morphology is also evident when looking at the images of cells liberated during thermal release (Figure 2.13); HepG2 cells form spheroids whereas the released HC04 hepatocytes are in the form of long, multi-layered cell sheets and in some instances the imprint of the non-woven fibre can be seen on the cell sheets. The disparity in the scaffold-associated HC04 cell numbers derived from the AB vs. DNA results may be attributable to differences in scaffold penetration of the respective reagents used. This discrepancy was not observed for HepG2 cells, which do not populate the matrix as densely and may allow for more uniform reagent diffusion.

The albumin assay indicated that the cell-lines are metabolically superior, when grown in 3D as compared to a conventional 2D monolayer, particularly in the case of HC04 cells. The comparison of 3D vs. 2D was carried out using an approximately 70% confluent 2D monolayer as this cell confluency is typically the benchmark used in conventional experimentation to represent the most optimal log phase of 2D hepatocyte growth. More mature, confluent 2D-cultured cells experience increased cellular stress and eventual cell death (39). Some fluctuation in albumin secretion was observed for both cell-lines, which is not unusual (39) and Glicklis *et al.* (126) also reported a decline in albumin production on day 7 in their 3D alginate scaffolds. Prestwich (82) suggests a possible cyclic production of albumin, as well as urea and EROD activity of hepatocytes (primary and HepG2-C3A cells) cultured on hydrogel surfaces or in 3D by encapsulation in Extragel, a synthetic extracellular matrix; our data suggests this to be accurate. HepG2 3D cultures had lower levels of albumin production as compared to HC04 3D cultures. This may be as a result of restrictions on mass transfer of essential nutrients caused by the formation of spheroids. This was observed by Dvir-Ginzberg *et al.* (127) when the spheroids in their alginate scaffolds reached sizes of 100 µm or larger. The compaction of the spheroids over time and the deposition of ECM proteins (127, 128) could lead to the decreased

Chapter 2: Hepatocyte proliferation and thermally induced cell detachment on 3D scaffolds

ability to remove cell secretions and reduce albumin levels in 3D HepG2 culture supernatants compared to the HC04 hepatocytes.

An additional indicator of superior hepatocyte growth on the scaffolds is increased CYP gene expression. Hepatocytes absorb drugs from the blood stream and metabolize them through phase-I and phase-II reactions (129). During phase-I metabolism, 90% of all drugs are oxidized by CYP isozymes with different substrate selectivity. Seven isoforms account for 95% of this activity namely 1A1, 1A2, 2C9, 2C19, 2D6, 2E1, and 3A4, with 3A4 responsible for over 65% of the metabolism of current therapeutic agents (82). Cytochrome isozymes are downregulated within 24 h after plating fresh hepatocytes onto conventional 2D tissue culture plastic (82), thus *in vitro* culture models that reflect the increased physiological CYP levels of primary hepatic tissues and cells are sought after in the pharmaceutical industry as surrogates for predicting *in vivo* phase I drug metabolism (130). In several instances the 3D non-woven scaffolds developed in this study promoted increases in CYP gene transcripts in both the HC04 and HepG2 cell-lines relative to their respective monolayers. Gene expression increased in a time-dependent manner for the HC04 cells grown on the 200 μm pore size scaffolds that had not been grafted with PNIPAAm. Expression of the *CYP2C9* and *CYP3A4* isoforms, however, remained below that of the 2D monolayer cells. Similarly, after 21 days of growth on the non-grafted scaffolds, HepG2 cells displayed increased expression of three out of six CYP isoforms compared to 2D monolayer cells, while the remaining isoforms had levels of gene expression equivalent or less than that observed for the 2D monolayer. This contrasts with the results observed for the scaffolds grafted with PNIPAAm. All the CYP genes tested demonstrated increased levels of expression as compared to the 2D control on scaffolds with pores sizes 100 μm and 150 μm . This is a good indication that the grafted layer serves not only as a mechanism for cell release from the scaffolds but positively influences hepatocyte growth and metabolism.

Two scaffolds with thermoresponsive properties were successfully developed, namely PP-*g*-PNIPAAm-A and PP-*g*-PNIPAAm-B. Large tracts of viable cells or spheroids were released from these scaffolds in a temperature-dependant manner and, by comparison with control scaffolds, this thermal release was shown to be exclusively caused by the grafted PNIPAAm layer. Fluorescent microscopy did, however, reveal that not all the cells were released from these thermoresponsive scaffolds. A comparison of thermal release versus trypsin treatment of the cells growing on scaffolds PP-*g*-PNIPAAm-B1 and PP-*g*-PNIPAAm-B2 revealed a similar efficiency in cell release from the scaffolds (Table 2.4). Scaffold PP-*g*-PNIPAAm-B3 however was more permissive to trypsin treatment possibly owing to the more open pore structure of the scaffold. The cells that remain in the scaffolds may either be trypsin resistant due to the 3D

Chapter 2: Hepatocyte proliferation and thermally induced cell detachment on 3D scaffolds

nature of the cell clusters and deposition of protective ECM proteins or may not be able to navigate out of the non-woven fibre network to be counted. Uneven grafting and scaffold areas devoid of PNIPAAm may be responsible for cells remaining on the scaffold. In addition, hepatocytes were, in some instances, observed to grow around the full circumference of the fibre, this means that when the phase transition of the PNIPAAm polymer triggers cell release it will simply repel the cells from the scaffold but will not be sufficient for the cells to separate from one another. It is for this reason that we believe some hepatocytes remain on the scaffold after the 2 h thermal release. Grafting efficiency and time for cell release are potential areas for further improvement. Currently the commercially available thermoresponsive 2D plates (UPCell™, Cell Seed Inc, Tokyo, Japan) require just over 30 min for release of a monolayer of cells.

In the preliminary design of the automated cell culturing system, the following criteria were identified: 1: the system should allow for the cultivation of large numbers of cells which would be achieved with a high surface area 3D scaffold; 2: it should allow for thermal, non-enzymatic cell release via the use of a thermoresponsive scaffold, thereby preserving the cell surface composition; 3: the proposed cell culturing system must be easy to operate with minimal human intervention required and 4: the automated culture system should be a small, cost-effective bench-top device that would be affordable to most cell culture laboratories.

Scaling up cell proliferation in the automated system revealed that it is possible to culture high numbers of cells on the non-woven scaffolds in the bioreactor. The cell numbers, however, are not sufficiently high to warrant using the automated system over conventional culturing if cell proliferation is the primary aim. Further optimisation to obtain cell numbers significantly higher than what can be obtained in culture flasks would be required. The proof-of-concept thermal release of cells from the grafted non-woven scaffolds was superior to that of the control non-woven scaffolds but this would need to be confirmed in a duplicate set of experiments.

This chapter demonstrated the proliferation and superior nature of hepatocytes growing on non-woven scaffolds in 3D. In the following chapter, selected scaffolds will be used to culture hepatocytes in 3D and once the hepatocytes have populated the scaffold, the hepatocytes will be infected with the liver stage (sporozoite) of the human malaria parasite *P. falciparum*. Invasion of sporozoites *in vitro* has historically been very challenging and we hypothesise that the more physiologically representative state the hepatocytes growing in 3D will enhance the permissiveness of the hepatocytes to the parasite. Although the data represented in Chapter 3 does not currently make use of the thermoresponsive properties of the scaffolds, this

Chapter 2: Hepatocyte proliferation and thermally induced cell detachment on 3D scaffolds

functionality may find an application in the future if the hepatocyte permissiveness to the malaria pathogen is indeed enhanced and researchers want to circumvent enzymatically removing the cells from the scaffolds in order to study surface antigens/proteins.